

# From Muscle to Text with MyoText: sEMG to Text via Finger Classification and Transformer-Based Decoding

MEGHNA ROY CHOWDHURY, Purdue University, USA

SHREYAS SEN, Purdue University, USA

YI DING, Purdue University, USA

Surface electromyography (sEMG) provides a direct neural interface for decoding muscle activity and offers a promising foundation for keyboard-free text input in wearable and mixed-reality systems. Previous sEMG-to-text studies mainly focused on recognizing letters directly from sEMG signals, forming an important first step toward translating muscle activity into text. Building on this foundation, we present MyoText, a hierarchical framework that decodes sEMG signals to text through physiologically grounded intermediate stages. MyoText first classifies finger activations from multichannel sEMG using a CNN-BiLSTM-Attention model, applies ergonomic typing priors to infer letters, and reconstructs full sentences with a fine-tuned T5 transformer. This modular design mirrors the natural hierarchy of typing, linking muscle intent to language output and reducing the search space for decoding. Evaluated on 30 users from the *emg2qwerty* dataset, MyoText outperforms baselines by achieving 85.4% finger-classification accuracy, 5.4% character error rate (CER), and 6.5% word error rate (WER). Beyond accuracy gains, this methodology establishes a principled pathway from neuromuscular signals to text, providing a blueprint for virtual and augmented-reality typing interfaces that operate entirely without physical keyboards. By integrating ergonomic structure with transformer-based linguistic reasoning, MyoText advances the feasibility of seamless, wearable neural input for future ubiquitous computing environments.

CCS Concepts: • **Human-centered computing** → **Empirical studies in ubiquitous and mobile computing**; • **Computing methodologies** → **Evolvable hardware**; **Neural networks**.

## ACM Reference Format:

Meghna Roy Chowdhury, Shreyas Sen, and Yi Ding. 2026. From Muscle to Text with MyoText: sEMG to Text via Finger Classification and Transformer-Based Decoding. *Proc. ACM Interact. Mob. Wearable Ubiquitous Technol.* 0, 0, Article 0 (2026), 25 pages. <https://doi.org/10.1145/nnnnnnn.nnnnnnn>

## 1 Introduction

Advances in wearable and ubiquitous computing are increasingly blurring the boundaries between humans and machines, enabling continuous, hands-free interaction across physical and virtual worlds [87]. As biosensing devices, which measure biological signals, grow smaller and integrate further into daily life, users need reliable, natural input methods that do not depend on specific surfaces [11]. Yet, common inputs like touchscreens, cameras, and motion sensors still rely on sight, lighting, or large gestures, limiting mobile and AR performance [78].

Among new input technologies, electromyography (EMG) offers a direct link to the body’s motor system by measuring electrical signals produced when muscles move [86]. Surface EMG (sEMG) captures these signals

---

Authors’ Contact Information: Meghna Roy Chowdhury, [mroycho@purdue.edu](mailto:mroycho@purdue.edu), Purdue University, West Lafayette, Indiana, USA; Shreyas Sen, [shreyas@purdue.edu](mailto:shreyas@purdue.edu), Purdue University, West Lafayette, Indiana, USA; Yi Ding, [yiding@purdue.edu](mailto:yiding@purdue.edu), Purdue University, West Lafayette, Indiana, USA.

---

Permission to make digital or hard copies of all or part of this work for personal or classroom use is granted without fee provided that copies are not made or distributed for profit or commercial advantage and that copies bear this notice and the full citation on the first page. Copyrights for components of this work owned by others than the author(s) must be honored. Abstracting with credit is permitted. To copy otherwise, or republish, to post on servers or to redistribute to lists, requires prior specific permission and/or a fee. Request permissions from [permissions@acm.org](mailto:permissions@acm.org).

© 2026 Copyright held by the owner/author(s). Publication rights licensed to ACM.

ACM 2474-9567/2026/0-ART0

<https://doi.org/10.1145/nnnnnnn.nnnnnnn>

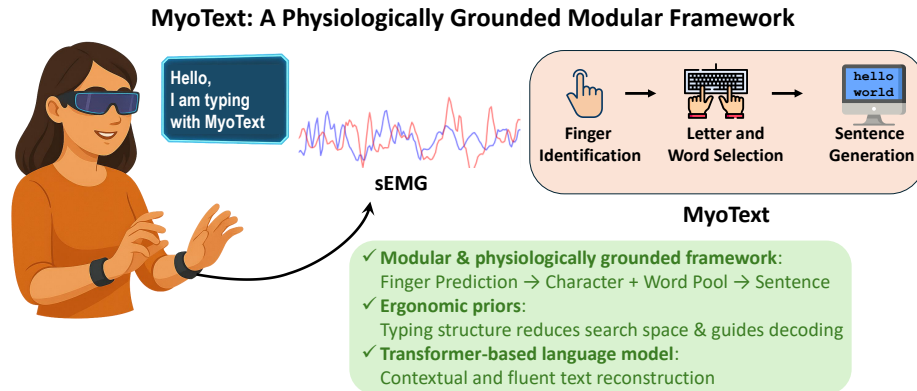


Fig. 1. **MyoText**. A physiologically-grounded modular sEMG-to-text decoding framework combining finger classification, ergonomic letter pooling, and sentence reconstruction.

non-invasively through skin-mounted electrodes [17, 21], supporting quiet and flexible interaction. These properties make sEMG useful in wearable and mixed-reality devices such as smartwatches, AR glasses, and neural wristbands [80, 86]. Recent systems like Meta Neural Band show that wrist-based sEMG sensors can recognize subtle finger motions for low-effort and discreet interactions [48, 54, 72]. These capabilities are important for AR and VR text input, enabling users to type in the air without physical keyboards. In such environments, decoding muscle activity through sEMG is an essential step toward achieving seamless text entry in extended reality (XR).

Despite this promise, realizing robust sEMG-to-text systems requires addressing three key challenges. First, sEMG signals naturally vary across users and sessions due to electrode placement, muscle fatigue, and individual anatomy [58, 60, 89, 93, 111]. Researchers have developed important stabilization techniques, including signal filtering, standardized electrode positioning, and per-user calibration, though achieving reliable cross-user generalization without calibration remains an open problem. Second, to handle this variability, the field has made progress through hierarchical decoding pipelines that first detect motion before classifying gestures or characters [14, 56], and through sequence models such as RNNs [43] and transformers [98] that capture temporal dependencies. These architectural advances have improved within-session stability, and scaling them to large, linguistically structured datasets represents the next frontier. Third, while foundational datasets like NinaPro (27 users) [68], MyoGym (12 users) [52], CSL-HDEMG (5 users) [3], and CapgMyo (18 users) [24], which are established for gesture recognition, continuous text-level decoding requires larger-scale data with naturalistic language structure. The *emg2qwerty* dataset [92] from Meta Reality Labs represents a major milestone, collecting annotated sEMG signals from 108 users during typing tasks. Participants were screened to ensure at least 90% correct finger-to-key mappings under standard QWERTY layout [8, 105, 114], capturing ergonomic typing behavior at scale. Using this dataset, the authors trained a convolutional neural network that maps sEMG activity directly to typed characters, achieving substantial character error rate (CER) improvements when augmented with a 6-gram language model. This result highlights an important insight: the strong reliance on linguistic priors suggests that direct character prediction from sEMG may not align with the physiological structure of the signal. sEMG naturally encodes finger-level muscle activations, motivating approaches that first decode fingers before resolving character ambiguity through ergonomic and linguistic constraints.

Building on this insight, we propose MyoText, a *physiologically grounded, modular* sEMG-to-text framework that models typing as a motor–linguistic hierarchy. As shown in Fig. 1, MyoText proceeds through three stages: (1) finger classification from sEMG signals, (2) ergonomically constrained letter and word pooling, and (3) transformer-based sentence generation. This design is motivated by three core principles. First, sEMG signals

naturally encode finger-level muscle activations, not abstract character identities. By predicting fingers rather than letters directly, MyoText aligns the decoding task with the physiological structure of the signal, reducing ambiguity and improving cross-user generalization. Second, typing ergonomics provides structural constraints that reduce the decoding search space. The standardized QWERTY finger-to-key mapping defines a natural prior that guides letter and word pooling, while remaining robust to non-canonical typing patterns through the downstream transformer. Third, separating motor decoding from linguistic reasoning improves both accuracy and deployability. Inspired by hierarchical decoding in brain-computer interfaces [14, 56], this modularity enables distributed execution, where the lightweight finger classifier can operate on resource-constrained wearables, while the transformer decoder can operate on resource-rich paired devices like smartphones [16].

We evaluate MyoText on the *emg2qwerty* dataset with 30 participants, selected for diversity and computational feasibility. MyoText achieves 85.4% finger classification accuracy and reconstructs sentences with a 5.4% Character Error Rate (CER) and 6.5% Word Error Rate (WER), substantially outperforming prior direct character prediction approaches. We further tested robustness under non-canonical finger-key mappings and linguistic variations, observing consistent decoding results.

To summarize, this work makes the following contributions:

- We introduce MyoText, a physiologically grounded, hierarchical sEMG-to-text decoding framework that separates motor intent from linguistic decoding through finger classification, ergonomic constraints, and a transformer-based sentence generation approach.
- We design a CNN-BiLSTM-Attention model for finger activation recognition and a constrained T5 decoder that achieves 85.4% finger prediction accuracy and 5.4% character error rate on *emg2qwerty*.
- We encode typing ergonomics as a structural prior that constrains the search space for transformer-based decoding and improves robustness to non-canonical finger-key mappings.
- We analyze the *emg2qwerty* dataset, revealing consistent finger-dependent sEMG structure and demonstrating generalization of MyoText through leave-one-user-out evaluation, cross-dataset testing on English corpora, and robustness under non-canonical typing patterns.

Together, these contributions advance sEMG-based text systems by showing that generalizable decoding is possible. By combining ergonomic design, modular architecture, and robust language models, this work establishes a practical and scalable foundation for sEMG-driven communication, paving the way for the future of the Internet of Bodies [88].

## 2 Background and Related Work

In this section, we first introduce the electromyography (EMG) biosignal and its underlying physiological principles. We then concentrate on the key applications of EMG in wearable devices, with a primary focus on sEMG-to-text decoding systems. Finally, we discuss the research gaps in current sEMGs-to-text studies.

**Electromyography (EMG).** Electromyography (EMG) is a physiological signal that captures the electrical activity produced by skeletal muscle activation, offering a direct interface to the human neuromuscular system [67]. EMG signals are generated by motor unit action potentials and are typically in the range of 1–10 mV, with dominant frequencies between 50–150 Hz [21]. These biopotential signals can be measured either invasively using needle electrodes, or non-invasively via surface EMG (sEMG) using skin-mounted electrodes [40]. While needle EMG offers clinical

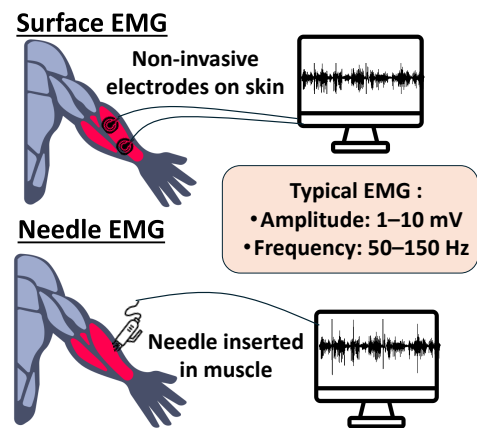


Fig. 2. EMG Sensing Modalities. Needle and surface EMG signal acquisition methods.

precision, sEMG is more widely adopted in wearable and mobile contexts due to its comfort, accessibility, and potential for integration with everyday interfaces [82]. Muscle tissue remains electrically quiescent at rest, but during contraction, it produces distinctive spatiotemporal patterns that encode motor intent [29]. These patterns form the basis for interpreting user actions and enabling responsive, intent-aware systems.

**sEMG with Wearable Devices.** Recent advances in wearable design have significantly improved the usability of sEMG-based systems [86]. These devices are now integrated into armbands, textiles, smart shoes, and gloves, spanning a wide range of platforms. Table 1 lists representative sEMG-enabled wearables and their application domains [22, 32, 34, 49, 56, 62, 81, 113]. Many of these devices support gesture recognition, mobility analysis, or rehabilitation, demonstrating the versatility of the sEMG signal in human-computer interaction. The latest advancement in sEMG wearables is the Meta Neural Band [72], a neural interface that decodes fine-grained motor intent from wrist-based sEMG with low-latency responsiveness. These developments illustrate sEMG’s transition from a clinical and biomechanical tool to a ubiquitous input interface, enabling next-generation typing and control paradigms.

**Applications of sEMG.** sEMG originated as a diagnostic tool for neuromuscular disorders, like muscular dystrophy, myasthenia gravis, and carpal tunnel syndrome [95, 96]. It then enabled myoelectric prostheses, where residual muscle signals provide intuitive control of artificial limbs [18, 97, 118]. As technology matured, sEMG expanded into sports medicine, rehabilitation, and ergonomics, using real-time muscle feedback to improve posture, reduce injury risk, and enhance performance [2, 19, 53, 107]. Applications span

wearable robotics, gait analysis, fall-risk monitoring, and studies of age-related sarcopenia [36, 42, 57, 70, 101]. Beyond physical applications, sEMG increasingly translates human intent into communication, where systems recognize sign-language gestures, supporting more natural interfaces for the deaf community, and assist individuals with partial paralysis or motor impairments by decoding intended movements into text or control commands [1, 9, 15, 28, 75, 94]. This sEMG-to-text trajectory captures muscle activity from the forearm, face, and larynx and maps it to written language or control signals [46, 47, 108]. sEMG is also integrated into immersive virtual environments, translating muscle intent directly into digital control [13, 25, 104]. The latest step is Meta’s sEMG neural-interface wristband, which detects subtle muscle signals and converts them into text and commands, advancing seamless, non-invasive interfaces for everyday communication and interaction [48, 54].

**Challenges with sEMG Signals.** Despite its growing appeal, sEMG signals present several technical challenges, particularly in dynamic real-world human-computer interaction. sEMG signals are naturally non-stationary and often exhibit low signal-to-noise ratios (SNR) [76]. Surface sEMG recordings are affected by various physiological and environmental factors, including electrical interference, motion artifacts, perspiration, shifting electrode contact, and user fatigue [27, 102]. Furthermore, sEMG captures aggregate activity from multiple overlapping muscle fibers, which can reduce signal specificity due to anatomical variability and inter-muscle crosstalk [5]. Even minor shifts in electrode placement between sessions can also result in substantial changes in signal patterns, complicating personalization and robust generalization across users.

Table 1. Summary of sEMG Wearable Devices.

Ref.	Form Factor	Application
[49]	Wearable Wristband	Gesture Recognition (Solar Powered)
[62]	Smart Footwear	Foot Gesture Recognition
[34]	Textile Shorts	sEMG Monitoring
[56]	Smart Socks	Leg Muscle Assessment
[32]	Robotic Glove	Hand Rehabilitation
[113]	Msleeve and Mbody Suit	Sports and Ergonomics
[81]	Myo Armband	sEMG Sensing for Gesture Control
[72]	Meta Neural Wristband	Neural Interface and Input Decoding

**Prior Work in sEMG-to-Text Input.** In this work, we focus on sEMG-to-text decoding. Prior research shows that this field has evolved through three main stages: from discrete keypress classification, to sequential gesture mapping, and finally to continuous text decoding from streaming signals. Early studies demonstrated that forearm sEMG signals can clearly distinguish individual keypresses. For example, Sharma et al. [90] extracted statistical features and used a k-nearest-neighbor classifier guided by reinforcement signals to reliably tell apart finger movements. Fu et al. [37] advanced this work by mapping coordinated three-finger gestures to a T9 layout; their CNN-LSTM model captured both spectral and temporal structures in multi-keypress sequences, moving beyond one-event-at-a-time recognition. Later, Crouch et al. [20] reframed EMG-based typing as a streaming sequence modeling problem, similar to speech recognition, generating text directly from overlapping muscle activity without explicit segmentation. Building on this idea, Sivakumar et al. [92] applied an automatic speech recognition-style model to the *emg2qwerty* dataset, using a time-depth separable CNN (with a 1s receptive field) and band-specific, rotation-invariant filters. They trained the model using Connectionist Temporal Classification (CTC) loss and decoded the outputs with a lexicon-free 6-gram character-level language model, employing modified Kneser-Ney smoothing and beam search. While these systems focus on replicating physical keyboard typing, the next step is to enable virtual keyboard text interaction, which motivates our approach in this work.

**Open Challenges in the State-of-the-Art.** Despite recent advancements, sEMG-to-text decoding continues to encounter challenges. sEMG signals are inherently noisy, vary across users, and often convey ambiguous information. Recent findings by Sivakumar et al. [92] demonstrated strong within-user accuracy but limited cross-user transfer. Fine-tuned personalized models achieved a 6.9% character error rate (CER) with a 6-gram language model, while generalized models (cross-user) reached a 51.78% CER. In the absence of a language model, CER increased to 11.28% and 55.38%, respectively, emphasizing the substantial reliance of current systems on language priors. These outcomes highlight the necessity for methods that generalize more effectively across users and leverage language models more efficiently. Future research should focus on developing models that learn transferable muscle-language representations with minimal calibration, directly capture local context from sEMG dynamics, and utilize the language model primarily for long-range support. The ultimate objective is to create on-body sEMG-to-text systems that remain comfortable, fast, and robust for continuous, keyboard-free typing.

### 3 Ergonomic Mapping of Letters to Fingers and the Variability

Building towards addressing the above-mentioned challenges and guide our design, we adopt an ergonomic letter-to-finger mapping that captures shared motor patterns and stabilizes decoding across users and sessions. We first infer the active finger from sEMG and then decode the letter within that finger's key set, which reduces the effective search space and supports virtual/keyboard-free operation while maintaining the language model as a lightweight long-range prior. The QWERTY keyboard layout naturally supports this approach. As the standard for English typing, it balances speed and comfort by minimizing finger movement [71]. As shown in Fig. 3(a), touch typing follows an ergonomic rule, each letter key belongs to one of eight fingers (excluding the thumbs) [8, 105, 114]. Typists place their fingers on the *home row*, ASDF for the left hand and HJKL for the right, and return there after each keystroke [103]. This habit limits motion, spreads effort evenly, and lets trained typists type faster with less mental effort because they no longer need to decide which finger to use. This mapping reflects long-standing conventions in typing training and is widely used in human-computer interaction and motor-control studies [84, 115, 116]. Research has shown that touch typists rely on consistent bimanual finger placement and kinesthetic feedback instead of visual cues [23], and trained typists build strong muscle-memory patterns that let them type without looking [39].

We apply the same rule to the *emg2qwerty* dataset by mapping each letter to one of these eight fingers (indexed 0–9, excluding thumbs). In Fig. 3(b), we find that common letters such as e, t, n, and o mostly come from the index and middle fingers (2, 3, 6), while rare letters like q, z, and p come from the pinkies (0, 9). This pattern

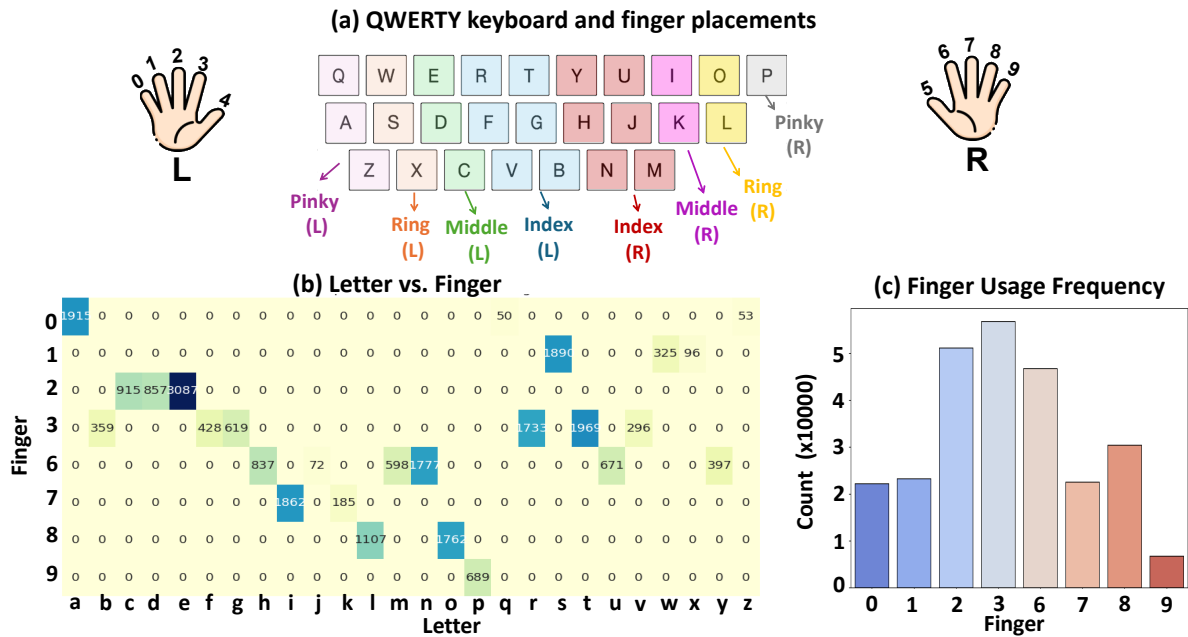


Fig. 3. **QWERTY Ergonomics and Finger Usage.** (a) The standard QWERTY keyboard layout is depicted, showing the conventional finger-to-key assignments. Letters are distributed among eight active fingers; the thumbs (4, 5) are included for completeness. (b) Finger-based letter mapping. (c) Finger usage frequency, highlighting dominance of index and middle fingers in the *emg2qwerty* dataset.

results in structured variation in the sEMG signals, where central fingers move more often and produce steadier signals, while edge fingers activate less often and exhibit greater variability. The finger-usage distribution in Fig. 3(c) confirms this asymmetry, reflecting both ergonomic design and meaningful physiological structure. We also acknowledge that many users deviate from canonical touch-typing (e.g., alternative fingerings, especially in the central keys of the keyboard). To account for this, our evaluation explicitly incorporates typing variability within *emg2qwerty* (§5.2.2 assessing performance across heterogeneous typing styles and non-canonical finger-letter assignments). Decoding models can use this finger-to-letter hierarchy as a built-in structure to reduce noise and generalize better across users and sessions. In short, the finger-based organization, anchored by the home row convention, acts as both a useful constraint and a strong prior for building robust decoders from sEMG signals.

#### 4 Proposed Methodology: The MyoText Framework

We present **MyoText**, a modular sEMG-to-text decoding framework that mirrors the structure of human typing behavior. As shown in Fig. 4, the MyoText framework has four steps: (i) *Data Preparation*, where we use sEMG signals from *emg2qwerty* dataset and align them with typed letters from a QWERTY keyboard, followed by mapping each letter to its corresponding finger based on typing ergonomics; (ii) *Finger-Level Classification*, where a Bi-LSTM with an attention mechanism is used to classify finger activity from the sEMG signals; (iii) *Letter Pooling and Candidate Word Construction*, where predicted fingers are mapped to candidate letters and used to generate plausible candidate words; (iv) *Sentence Prediction via Transformer-Based Decoding*, where a fine-tuned T5-based transformer language model decodes candidate words into syntactically and semantically plausible sentences. In the following subsections, we detail the design of each step of MyoText.

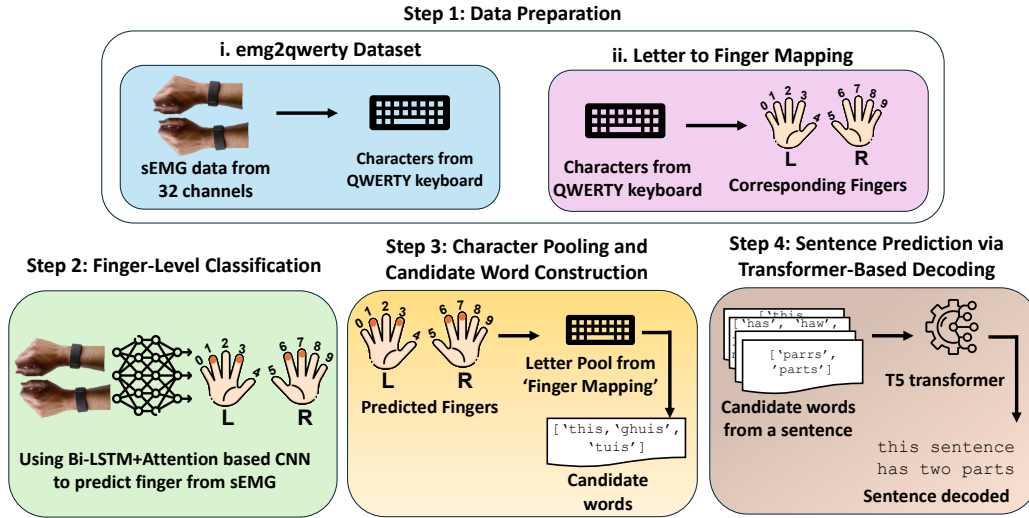


Fig. 4. **MyoText: Modular sEMG-to-Text Framework.** The four-stage diagram from sEMG signals to sentence decoding: (i) data preparation with ergonomic finger mapping, (ii) finger classification, (iii) letter & candidate word pooling, and (iv) T5-based decoding.

#### 4.1 Data Preparation

We start by extracting time-aligned sEMG segments for each keypress from the raw HDF5 logs in the *emg2qwerty* dataset [30]. Although this process is designed for *emg2qwerty*, our modular pipeline can easily adapt to other datasets or preprocessing setups. Each log records synchronized sEMG signals from 32 electrodes (16 on each forearm) along with timestamps for every keystroke. For each keypress, we match the recorded key and its timestamp to locate the corresponding sEMG interval, and then extract a short segment that includes 1s before and after the event to capture both preparatory and residual muscle activity. We keep all 32 channels at their original resolution and save the processed segments as compressed files to speed up later analysis.

Next, we label each letter with the finger that typically presses it, following standard typing ergonomics [8, 105, 114] and the QWERTY keyboard layout [71]. We map letters to eight active fingers (indices 0–3 for the left hand and 6–9 for the right) while reserving the thumbs for the spacebar. Table 2 shows the full key-to-finger mapping. Although not every user follows the exact QWERTY convention, prior studies in typing biomechanics and sEMG research have used this mapping as a consistent baseline. Classic ergonomics work measured fine-wire sEMG signals from ten expert typists [33], and later studies continued to recruit experienced typists for controlled experiments [27, 91, 112]. The *emg2qwerty* dataset [92] also screened participants to ensure they could type without looking at the keyboard and follow the correct finger-to-key mapping at least 90% of the time. This consistency supports the continued use of standardized mappings in sEMG-based typing research. To verify how well our method handles user variation, we also added controlled perturbations to the finger-to-key mapping during evaluation to test robustness (see §5.2.2). The results show that even when users deviate from the standard mapping, our method maintains strong performance, confirming its robustness to individual typing styles.

Table 2. Letter to Finger Mapping

Left Hand			Right Hand		
Key	Finger	#	Key	Finger	#
a	Pinky (L)	0	n	Index (R)	6
b	Middle (L)	3	o	Ring (R)	8
c	Middle (L)	2	p	Pinky (R)	9
d	Middle (L)	2	h	Index (R)	6
e	Middle (L)	2	u	Index (R)	7
f	Index (L)	3	i	Middle (R)	7
g	Index (L)	3	j	Index (R)	6
q	Pinky (L)	0	k	Middle (R)	7
r	Index (L)	3	l	Ring (R)	8
s	Index (L)	1	y	Index (R)	6
t	Index (L)	3	m	Index (R)	6
v	Index (L)	3			
w	Ring (L)	1			
x	Ring (L)	1			
z	Pinky (L)	0			

**Step 1 (ii): Letter to Finger Mapping**

Characters from QWERTY keyboard → Corresponding Fingers (L, R)

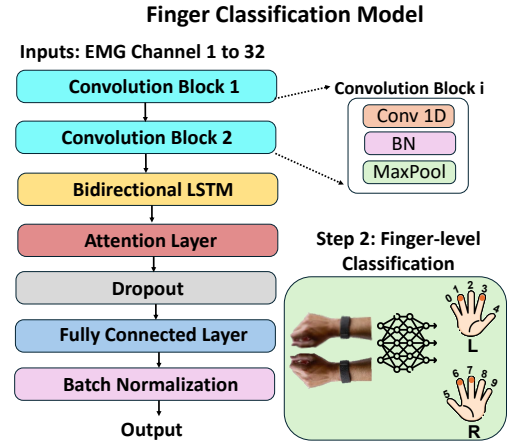


Fig. 5. Finger Classification Network. CNN–BiLSTM–Attention architecture for predicting finger labels from multichannel sEMG.

## 4.2 Finger-Level Classification

Given the extracted (sEMG segment, finger label) pairs, we train a model that predicts which finger generates each muscle signal directly from the raw multichannel sEMG input. By framing the task at the finger level instead of the letter level, we reduce the classification space from 26 letters to 8 fingers, thereby better matching how real muscle activations occur during typing. This design helps the model handle problems such as letter-level class imbalance and overlapping muscle activity between letters, making it more robust and easier to generalize to new users.

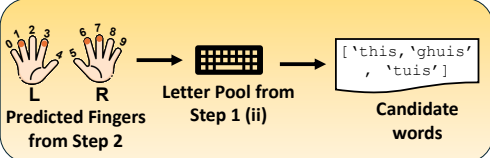
The finger-level classification is a supervised learning problem with two goals: (i) capture short-term correlations across multiple sEMG channels, and (ii) model bidirectional temporal dependencies, since muscle activations often include both anticipatory and residual signals. We use CNNs to learn local spatiotemporal features and LSTMs to track longer dependencies in both time directions [31, 59, 83]. Building on these strengths, our model stacks convolutional blocks followed by a bidirectional LSTM layer. We also incorporate an attention mechanism to highlight the most informative time steps, and fully connected layers refine the representation to predict the correct finger class. In short, our architecture combines CNN, BiLSTM, and attention modules with fully connected layers for final classification (Fig. 5).

The model takes an input sequence  $\mathbf{X} \in \mathbb{R}^{C \times T}$ , where  $C$  is the number of electrode channels and  $T$  is the number of time steps, and outputs the predicted finger label  $y \in \{0, \dots, 7\}$ . The architecture runs through four stages in sequence:

- **Convolutional feature extraction.** A convolutional layer applies  $\mathbf{H}^l = \sigma(\mathbf{W}^l * \mathbf{H}^{l-1} + \mathbf{b}^l)$  with  $\mathbf{H}^0 = \mathbf{X}$ , where  $*$  denotes the convolution operation,  $\sigma$  is the ReLU activation, and  $\mathbf{W}^l, \mathbf{b}^l$  are trainable kernels and biases. Each convolutional filter learns to detect localized temporal features in the sEMG waveform. Max-pooling reduces the temporal dimension from  $T$  to  $T'$ . This stage thus encodes short-term dependencies and frequency-specific energy variations related to motor unit recruitment.

Table 3. Examples of Finger-to-Letter Mapping and Word Candidate Pooling.

**Step 3: Letter Pooling and Candidate Word Construction**



Letter	Predicted finger	Letter pool	Candidate words
t	3	b f g r t v	
h	6	h j m n u y	['ghis', 'this', 'tuis']
i	7	i k	
s	1	s w x	

- Temporal modeling with BiLSTM.** The convolved features  $\mathbf{H}^L \in \mathbb{R}^{F \times T'}$  (where  $F$  is the number of learned feature maps) are passed to a bidirectional LSTM to model long-range temporal dependencies. The forward update  $\vec{\mathbf{h}}_t = \text{LSTM}_f(\vec{\mathbf{h}}_{t-1}, \mathbf{H}_t^L)$  captures past context, while the backward update  $\overleftarrow{\mathbf{h}}_t = \text{LSTM}_b(\overleftarrow{\mathbf{h}}_{t+1}, \mathbf{H}_t^L)$  captures future context. The concatenated hidden state  $\mathbf{h}_t = [\vec{\mathbf{h}}_t; \overleftarrow{\mathbf{h}}_t]$  encodes bidirectional temporal information, preserving both anticipatory and residual activity. This is crucial for sEMG, where muscle activation and relaxation phases often overlap, and motion intent can be inferred from both preceding and succeeding signal dynamics.
- Attention-based focus.** To emphasize physiologically informative segments, the model learns an attention distribution over time. Each BiLSTM output  $\mathbf{h}_t \in \mathbb{R}^{d_h}$  represents a  $d_h$ -dimensional hidden feature vector capturing the temporal EMG context at time  $t$ , including contraction intensity and transition dynamics. The model computes a relevance score  $e_t = \mathbf{v}^\top \tanh(\mathbf{W}_a \mathbf{h}_t)$ , where  $\mathbf{W}_a \in \mathbb{R}^{d_a \times d_h}$  is a trainable projection matrix mapping hidden states into an attention space, and  $\mathbf{v} \in \mathbb{R}^{d_a}$  is a context vector that measures their physiological relevance. The normalized weight  $\alpha_t = \exp(e_t) / \sum_{t'} \exp(e_{t'})$  quantifies the contribution each time, and the context vector  $\mathbf{c} = \sum_t \alpha_t \mathbf{h}_t$  aggregates features proportionally to their learned importance.
- Fully connected layers.** The context vector  $\mathbf{c} \in \mathbb{R}^{d_c}$  is passed through a dense layer with ReLU to compute  $\mathbf{z} = \phi(\mathbf{W}_f \mathbf{c} + \mathbf{b}_f)$ , followed by dropout and batch normalization. The classifier output is  $\hat{\mathbf{y}} = \text{softmax}(\mathbf{W}_o \mathbf{z} + \mathbf{b}_o)$  with  $y \in \{0, \dots, 7\}$ ,  $\hat{y}_k \in [0, 1]$ , and  $\sum_{k=0}^7 \hat{y}_k = 1$ ; for  $K = 8$  classes, the cross-entropy loss is  $\mathcal{L} = -\sum_{k=0}^{K-1} \mathbb{1}[y = k] \log \hat{y}_k = -\log \hat{y}_y$ . Where:  $\phi$  is ReLU;  $\mathbf{z} \in \mathbb{R}^{d_z}$ ;  $\mathbf{W}_f \in \mathbb{R}^{d_z \times d_c}$ ,  $\mathbf{b}_f \in \mathbb{R}^{d_z}$ ;  $\hat{\mathbf{y}} \in \mathbb{R}^K$  with  $K = 8$ ;  $\mathbf{W}_o \in \mathbb{R}^{K \times d_z}$ ,  $\mathbf{b}_o \in \mathbb{R}^K$ ;  $y$  is the ground-truth class index;  $\hat{y}_k$  is the predicted probability for class  $k$ ;  $\mathbb{1}[y = k]$  is the indicator function. Note: if  $\mathbf{c} = \sum_t \alpha_t \mathbf{h}_t$  directly, then  $d_c = d_h$ .

This model combines convolutional blocks, BiLSTM units, attention, and fully connected layers to blend local spatial features with temporal and contextual information. It aligns the classification task with how people type, grounding the architecture in real muscle and finger movements. As a result, the model can learn multichannel sEMG signals and predict which finger is active. These finger predictions then feed into the next stage of the MyoText pipeline, where the system maps fingers to possible letters and begins reconstructing words.

### 4.3 Letter Pooling and Candidate Word Construction

After predicting which finger produced each keystroke, we restrict the letter search space using a fixed mapping from fingers to letter subsets based on the standard QWERTY touch-typing layout. Table 3 lists some examples of the finger-to-letter mapping. For instance, finger index three maps to letters including b, f, g, r, t, and v, which people normally type with the left index finger. This step both reduces the decoding search space and adds biomechanical knowledge to the prediction process, making the model faster and more realistic. For each predicted finger sequence for a word (e.g., *this*  $\rightarrow$  [3, 6, 7, 1]), we map each finger to its corresponding set of possible letters to produce a *letter pool sequence* that lists possible letters for each position in the word.

Table 4. Examples of Candidate Word Pools Using Finger-Based Letter Pools.

Sentence	Letter Pool Sequence	Candidate Words
this	[b f g r t v ; h j m n u y ; i k ; s w x]	ghis, this, tuis
has	[h j m n u y ; a q z ; s w x]	has, haw, jaw, mas, max, naw, yas, yaw
two	[b f g r t v ; s w x ; l o]	two
parts	[p ; a q z ; b f g r t v ; b f g r t v ; s w x]	parrs, parts
legitimate	[l o ; c d e ; b f g r t v ; i k ; b f g r t v ; i k ; h j m n u y ; a q z ; b f g r t v ; c d e]	legitimate
load	[l o ; l o ; a q z ; c d e]	load, ooze
economic	[c d e ; c d e ; l o ; h j m n u y ; l o ; h j m n u y ; i k ; c d e]	economic
women	[s w x ; l o ; h j m n u y ; c d e ; h j m n u y]	soncy, women, wouch

From this letter pool sequence, the next step is to build *candidate word pool*. The idea first to take the Cartesian product of all letter pools to generate every possible word combination, and then filter these words using large English corpora such as the Brown Corpus [69], WordNet [73], and public English dictionaries [26]. This filtering step removes invalid or nonsensical combinations (e.g., “bbs”, “jnd”) while preserving real English words. Table 4 shows examples of the resulting candidate word pools.

#### 4.4 Sentence Prediction via Transformer-Based Decoding

In the final stage of our framework, we build complete sentences from the candidate word pools. The first-stage finger classification introduces some level of uncertainty, which can propagate to the word pools. To handle this, the sentence decoder should examine the entire sentence instead of focusing only on nearby words. Therefore, we utilize a transformer-based language model that processes all candidate sets simultaneously and selects one word from each set to form the final, coherent sentence.

**T5 Transformer.** We use the Text-to-Text Transfer Transformer (T5) introduced by Google in 2019 [77]. T5 was pretrained on the Colossal Clean Crawled Corpus (C4) with a vocabulary size  $|\mathcal{V}| \approx 32,000$ . The T5 model includes an encoder and a decoder. The encoder has multiple layers (e.g., 12 in T5-Base), each with bidirectional self-attention, a two-layer feed-forward network with ReLU activation, layer normalization, and residual connections for stable training. The decoder mirrors this structure but adds masked self-attention to avoid looking at future tokens and includes encoder–decoder attention for contextual generation [77]. T5 is a general sequence-to-sequence model that can be fine-tuned for tasks such as summarization, question answering, and text classification [6, 7, 61, 64, 106, 117]. Its scalability and strong performance on benchmarks such as GLUE and SuperGLUE [109, 110] have made it widely used in downstream applications.

We choose T5 for our sentence decoding task because its encoder–decoder structure enables global reasoning across the entire sentence. The encoder captures bidirectional context from the input sequence, while the autoregressive decoder generates text by conditioning on both the encoder outputs and previously generated tokens. This design lets the model use later context to fix earlier uncertainties. For example, distinguishing “has” from “haw” when it processes the phrase “two parts”, which is essential for accurate decoding in MyoText.

**Input Representation Adaptation.** Unlike typical sequence-to-sequence tasks where the input is already a token sequence, MyoText’s sentence decoder takes structured candidate word pools (after Step 3). Standard T5 cannot directly process such structured inputs because it expects a flat text sequence. To address this, we turn a sequence of candidate word pools  $\mathcal{G}_1, \dots, \mathcal{G}_N$  (where  $N$  is the sentence length) into an instruction-based prompt of

Table 5. Examples of Using Candidate Word Pools to Generate Sentences.

Sentence	Candidate Pool	Data representation	Decoded Sentence
this has two parts	ghis this tuis ; has haw jaw mas maw max naw yas yaw ; two ; parrs parts ;	Select exactly 4 words: ghis this tuis <SEP> has haw jaw mas maw max naw yas yaw <SEP> two <SEP> parrs parts <SEP>	this has two parts
legitimate load economic women	legitimate ; load ooze ; economic ; soncy women wouch ;	Select exactly 4 words: legitimate <SEP> load ooze <SEP> economic <SEP> soncy women wouch <SEP>	legitimate load economic women
card resolve issues voters	cafe cage card care cate cave dard dare date dave eave ; resolve ; issues ; borers gofers rogers rovers toters voters ;	Select exactly 4 words: cafe cage card care cate cave dard dare date dave eave <SEP> resolve <SEP> issues <SEP> borers gofers rogers rovers toters voters <SEP>	<b>cage</b> resolve issues voters

**Step 4: Sentence Prediction via Transformer-Based Decoding**

Example text from emg2qwerty dataset → Candidate Pool

Candidate words from a sentence (['parrs', 'parts']) → T5 transformer → Sentence decoded (this sentence has two parts)

string using a delimiter token <SEP> for separation, i.e., “Select exactly  $N$  words:  $\mathcal{G}_1$  <SEP>  $\mathcal{G}_2$  <SEP> ...  $\mathcal{G}_N$  <SEP>”. This constrains that at position  $n$ , MyoText only allows choices from the corresponding candidate word pool. For example, in column 3 of Table 5, the sentence “this has two parts” with candidate word pools  $\mathcal{G}_1 = \{\text{ghis, this, tuis}\}$ ,  $\mathcal{G}_2 = \{\text{has, haw}\}$ ,  $\mathcal{G}_3 = \{\text{two}\}$ ,  $\mathcal{G}_4 = \{\text{parrs, parts}\}$  produces the serialized input  $S = \phi(\mathcal{G}_1, \dots, \mathcal{G}_4)$ : “Select exactly 4 words: ghis this tuis <SEP> has haw <SEP> two <SEP> parrs parts <SEP>”.

**Sentence Generation via Constrained Beam Search.** We integrate beam search with a fine-tuned T5 model to generate sentences from the candidate word pools. T5’s encoder reads the adapted serialized input string once and produces contextual embeddings that represent all possible words jointly. During decoding, T5 generates the sentence word by word. At each position  $n$ , T5 only considers words from the corresponding candidate pool  $\mathcal{G}_n$  as valid options. For each candidate word, we compute its probability under the T5 decoder, conditioned on both the encoder context and the words already chosen. Beam search then maintains a set of the top- $B$  (where  $B$  is the beam width) partial sentences, expands each one with all candidate words in  $\mathcal{G}_n$ , and retains the highest-scoring continuations. After all positions are filled, MyoText selects the sentence with the best total score. This process enables T5 to apply its global language knowledge from pretraining while beam search systematically explores and scores multiple word combinations, producing a final sentence that is both fluent and consistent with the physiological decoding constraints. Column 4 of Table 5 lists examples of the decoded sentences from candidate word pools.

## 5 Evaluation

In this section, we evaluate MyoText. We report finger-level classification accuracy, sentence-level error (CER/WER), robustness to typing variability and cross-dataset shift, and end-to-end comparisons with prior sEMG-to-text systems. We also analyze the *emg2qwerty* dataset to assess signal quality. Unless otherwise noted, all experiments use the *emg2qwerty* dataset. We address the following research questions (RQs):

- **RQ1:** What is the performance of MyoText’s modular decoding framework, from finger-level classification to sentence generation?
- **RQ2:** How well does MyoText generalize to longer, naturalistic text and non-canonical typing patterns?
- **RQ3:** Does the *emg2qwerty* dataset provide sufficient scale and keystroke-level alignment to serve as a reliable benchmark for sEMG-to-text decoding?
- **RQ4:** How does MyoText position itself within the evolution of sEMG-to-text systems, and what insights does it provide for deployment?

### 5.1 RQ1: Performance of MyoText

We evaluated MyoText using the *emg2qwerty* dataset because it is the most diverse sEMG-to-text dataset available released in 2024 [92]. It consists of synchronized sEMG recordings from both forearms (16 channels per side) along with annotated keystroke events. We extracted structured examples containing the user ID, keystroke timing, and the multi-channel sEMG segments. This ensures that every keystroke is paired with its corresponding sEMG window. The data preprocessing pipeline was run on Google Colab using CPU resources and took about 15 hours to complete. In total, we evaluated using data from 30 participants. For finger classification, we trained the neural network model with the Adam optimizer [50] (learning rate  $10^{-3}$ , batch size 32) for 100 epochs. To prevent overfitting, we applied a combination of regularization strategies, including an adaptive learning rate scheduler (ReduceLRonPlateau [100] with a decay factor of 0.01 when the validation loss plateaued) and early stopping with a patience of 10 epochs. For sentence decoding, we fine-tuned a pretrained T5 transformer [77] using teacher forcing. Fine-tuning was performed with a batch size of 32, a learning rate of  $5 \times 10^{-5}$  for up to 30 epochs using the Hugging Face Trainer API. All models were implemented in TensorFlow, with pretrained models imported from Hugging Face [99]. Training and fine-tuning were conducted on either an NVIDIA T4 or an NVIDIA L40, depending on availability on Google Colab.

**5.1.1 Finger-Level Classification.** A key design choice in MyoText is whether to classify finger activations (8 active fingers) first or directly predict letters (26 classes) as the final output. An RNN-based approach is a natural fit for this problem, as recurrent models such as LSTMs are widely used for time-series decoding and can effectively capture temporal dependencies in sEMG signals. Our preliminary experiments showed that averaging left and right arm signals into two input channels significantly degraded performance (40.3% accuracy) due to the loss of spatial detail. In contrast, using the full 32-channel input in the same CNN-LSTM architecture improved accuracy to 71.2%, underscoring the importance of high-resolution sEMG representation. Hence, we trained two variants of the same CNN-BiLSTM-Attention architecture (§4.2), differing only in their output targets:

- Model 1 (Finger Classification): Predicts 8 finger labels; achieves 85.4% average accuracy.
- Model 2 (Letter Classification): Predicts 26 letters directly; achieves 51.2% average accuracy.

This performance gap highlights the tractability of finger-level decoding. sEMG signals are activated due to finger activity, and hence tend to cluster by finger activation rather than by individual letters, since multiple keys share similar muscular patterns when typed by the same finger. This overlap makes letter-level classification significantly more ambiguous. Fig. 6 illustrates this contrast. The confusion matrix for Model 1 (Fig. 6a) shows clear diagonal dominance, indicating clean finger

Table 6. **Finger vs. Letter Variant Accuracy (BiLSTM+Attn).**

Fold	Model 1 (%)		Model 2 (%)	
	CV	LOUO	CV	LOUO
1	82.71	85.52	43.85	29.76
2	82.01	85.41	47.52	28.46
3	88.66	80.98	51.2	30.84
4	89.30	78.84	54.87	25.52
5	84.61	77.27	58.55	26.73
<b>Mean ± Std</b>	<b>85.45 ± 3.36</b>	<b>81.4 ± 3.76</b>	<b>51.2 ± 5.81</b>	<b>28.5 ± 2.25</b>

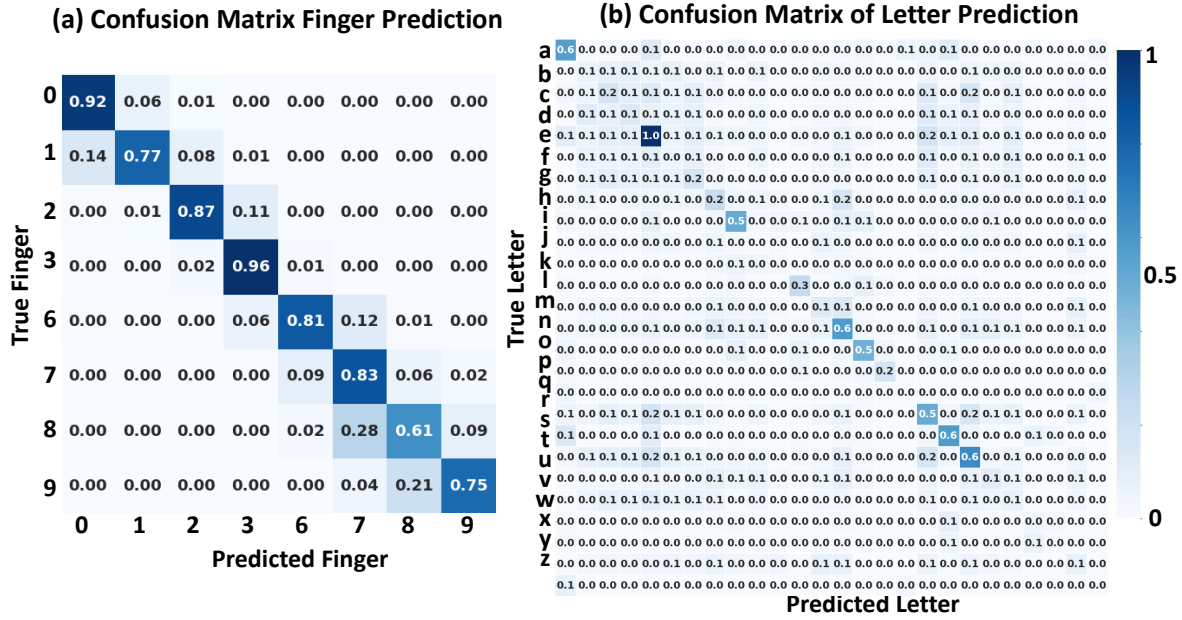


Fig. 6. Confusion matrices: Finger vs. Letter Prediction (a) Model 1 (b) Model 2

separation. In contrast, Model 2’s confusion matrix (Fig. 6b) reveals substantial misclassifications, particularly among spatially adjacent keys (or those involving similar muscular activations). We further evaluated the models’ robustness using two validation protocols. As shown in Table 6, 5-fold cross-validation yields an average accuracy of  $85.45\% \pm 3.36\%$ , while leave-one-user-out (LOUO) validation on five held-out users achieves  $81.4\% \pm 3.76\%$  on Model 1. The results of Model 2 are shown in the same table. *While our models follow the standard QWERTY finger-to-key mapping (Table 2), there may be user-specific deviations like typing ‘B’ with the right index finger instead of the left. We consider such scenarios in §5.2.2, and our downstream transformer decoder effectively resolves these inconsistencies using sentence-level context, ensuring robustness to both finger prediction errors and real-world typing variability.*

**5.1.2 Sentence-Level Prediction.** Following finger classification, we decode candidate word pools (§4.3) into complete sentences using a fine-tuned T5 transformer [77]. Sentence reconstruction performance is evaluated using Word Error Rate (WER) and Character Error Rate (CER), defined in Equations 1 and 2, where  $S$ ,  $D$ , and  $I$  represent substitutions, deletions, and insertions, and  $N$  is the total number of reference words or characters.

$$\text{WER} = \frac{S_W + D_W + I_W}{N_W} \quad (1)$$

$$\text{CER} = \frac{S_C + D_C + I_C}{N_C} \quad (2)$$

**Model Variants and Results.** We evaluate three T5-base variants, each trained on the candidate-to-sentence generation task:

- **T5 Model 1:** Baseline with standard cross-entropy loss ( $\mathcal{L}_{M1} = \mathcal{L}_{CE}$ ).
- **T5 Model 2:** Adds a substitution-aware auxiliary loss ( $\mathcal{L}_{M2} = \mathcal{L}_{CE} + \lambda \mathcal{L}_{aux}$ ).

- **T5 Model 3:** Incorporates Model 2’s loss, plus weight decay, label smoothing, and early stopping.

Fig. 7 shows that T5 Model 3 achieves the best performance, with 6.5% WER and 5.4% CER. These results indicate that the decoder effectively leverages sentence-level context to overcome noise from finger-level predictions and candidate ambiguity.

**Error Analysis.** Table 7 presents representative decoding errors. Most fall into three categories: (i) semantically or phonetically similar substitutions (e.g., “card” → “cage”), (ii) omitted proper nouns (e.g., “Uzbekistan”, “Moldova”), and (iii) early termination or truncation.

While average WER and CER are low, we observe a standard deviation of approximately 7%. This variance is largely attributable to the nature of the *emg2qwerty* dataset, which includes short and syntactically sparse phrases. In such cases, even a single word error can disproportionately affect WER (e.g., 25% WER for a 4-word sentence with one incorrect word). Nonetheless, the model generally preserves sentence length and fluency, even when lexical accuracy varies. Despite upstream errors introduced by finger misclassifications or variability in finger-to-key mappings, the transformer-based decoder consistently, hence supporting our modular framework.

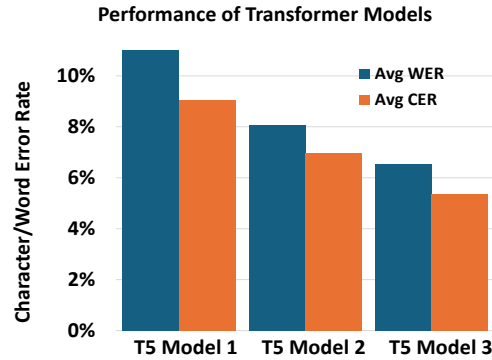


Fig. 7. **T5 Model Performance.** CER and WER across T5 variants. Lower is better.

Table 7. **Comparisons between Reference and Predicted Sentences in the emg2qwerty dataset.**

SI No.	Reference <sup>#</sup>	Prediction <sup>*</sup>
1	the quick brown fox <b>jumps over</b> a lazy dog	the quick brown fox a lazy dog ▲
2	court financing <b>allen</b> sisters	court financing <b>all</b> sisters ★+
3	<b>card</b> resolve issues voters	<b>cage</b> resolve issues voters +
4	dealt extraction <b>somebodys</b> purchasing	dealt extraction purchasing ▲
5	olympic <b>moldova</b> rock corpus	olympic rock corpus ★ ▲
6	spine retain <b>shed</b> fever	spine retain <b>shee</b> fever +
7	<b>Uzbekistan</b> employ utah british	employ utah british ★ ▲
8	suspected possible penny <b>handhelds</b>	suspected possible penny ▲
9	across <b>changelog</b> petition raised	across petition raised ▲
10	charger <b>denver</b> reflected widescreen	charger reflected widescreen ★ ▲
11	<b>tuesday</b> lithuania independent wrap	<b>thesean</b> lithuania independent wrap ★+

**Error Type:** + Word Substitution ▲ Missing word(s) ★ Proper noun / Phonetic confusion

**\*Prediction is based on Candidate Word Construction (Step 3) which is in-turn generated by Finger-Level Classification (Step 2) ; # Sentences are ground truth from emg2qwerty**

Table 8. Comparisons between Reference and Predicted Sentences using Natural English Sentences.

Reference	Prediction
a girl lives in <b>a</b> small town	a girl lives in small town <b>Missing word 'a'</b>
she goes to the farm every day	she goes to the farm every day
the farm is near her home	the farm is near her home
she feeds the cows	she feeds the cows
she gives them grass and water	she gives them grass and water
the cows like her	the cows like her
one day a cow is sick	one day a cow is sick
the girl tells her father	the girl tells her father
he calls a doctor	he calls a doctor
the doctor helps the cow	the doctor helps the cow
the girl is happy	the girl is happy

**Note: The prediction is based on T5 Model 3 only; there is no Finger-Level Classification here**

### Key Takeaway from RQ1

On *emg2qwerty*, MyoText reaches 85.4% finger classification and 5.4% sentence CER via a three-stage modular framework aligned with motor→ergonomic→linguistic structure: (1) *Finger*: sEMG classifies fingers better than letters (direct letters: 51.2%). (2) *Ergonomics*: QWERTY finger–key constraints cut the per-position search depending on the standard finger-to-letter mapping. (3) *Sentence Generation*: a T5 decoder resolves residual ambiguity, yielding coherent sentences without per-user calibration.

## 5.2 RQ2: Generalization Under Real-World Typing and Sentence Variability

A key requirement for practical sEMG-to-text decoding is the ability to generalize beyond the constraints of the training dataset. While *emg2qwerty* serves as an important first benchmark for sEMG-to-text research, it remains limited in both linguistic diversity and typing variability. To assess broader generalization, we evaluate our approach in three settings: (i) sentence-level decoding on naturalistic, paragraph-scale text, (ii) robustness to deviations from canonical finger-to-key mappings, and (iii) cross-domain evaluation using open-source text datasets with simulated typing variability, since no open-source sEMG-to-sentence datasets currently exist.

**5.2.1 Natural Language Generalization.** To evaluate whether the sentence decoder overfits to the short, syntactically sparse structures in *emg2qwerty* (mean sentence length  $\approx 4$  words), we tested the best-performing transformer model (T5 Model 3) on a paragraph of declarative English sentences, each of similar length, generated via ChatGPT-4. This evaluation isolates the language model’s capability using candidate word pools only; no sEMG signals or finger classification are involved. As shown in Table 8, the sentence decoder reconstructs long-form sentences with near-perfect fidelity. The only deviation is a minor article omission (“a girl lives in a small town” → “a girl lives in small town”),

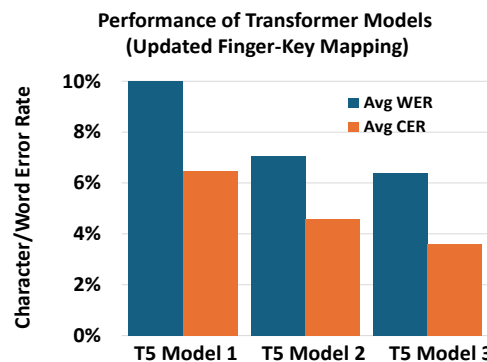


Fig. 8. Decoding Performance of T5 Variants as mentioned in RQ1 with Updated Letter Pool. Lower the CER and WER indicates better performance.

Table 9. **Augmented Finger-to-Letter Mappings.** Canonical QWERTY pools are extended with additional letters to reflect plausible typing deviations, to simulate user variability, and evaluate robustness.

Finger (Left)	Updated Letter Pool	Finger (Right)	Updated Letter Pool
Pinky (0)	[q, a, z]	Pinky (9)	[p]
Ring (1)	[w,s,x]	Ring (8)	[o, l]
Middle (2)	[e,d,c,w,s,x]	Middle (7)	[i,k,o,l,p]
Index (3)	[r,f,v,t,g,b]	Index (6)	[y,h,n,u,j,m,t,g,b]

resulting in a WER of 1.43% and CER of 0.41%. These results confirm that the model generalizes well and does not memorize fixed phrase structures.

**5.2.2 Robustness to Typing Variability.** While the QWERTY layout defines a canonical finger-to-key mapping, real-world typing often diverges, particularly for centrally located keys. For instance, the letter b, typically assigned to the left index finger (Finger 3), is frequently typed with the right index (Finger 6); similarly, x, s, and w may shift from the left ring (Finger 1) to the left middle finger (Finger 2), and o, l, and p are often typed with the right middle (Finger 7) instead of the right ring or pinky. To capture such variation, we augmented the candidate letter pools with plausible alternatives based on observed typing behavior (Table 9). This introduces realistic ambiguity into decoding, simulating behavioral noise. We re-evaluated all T5 models (Models 1–3) on *emg2qwerty* using these expanded pools, keeping all other pipeline components unchanged. As shown in Fig 8, performance remains similar, with only minor increases in CER and WER. These findings confirm that MyoText generalizes not only linguistically but also behaviorally, preserving decoding fidelity under realistic finger-to-key variation. This robustness supports its deployment across diverse user typing styles and input conditions.

**5.2.3 Cross-Dataset Generalization.** A key application of our method is in AR/VR systems, such as Meta’s Neural Band and Ray-Ban Display [45], where typing is primarily used for short-form communication (e.g., texting). To assess generalization beyond *emg2qwerty*, we evaluated the sentence decoder on two public corpora from Kaggle [10, 79], denoted D1 (chat sentiment; 741 sentences) and D2 (random English sentences; 584 sentences).

While these datasets do not contain sEMG recordings, they are used to evaluate the sentence decoder’s linguistic generalization under simulated input variability. Finger-level perturbations, derived from the augmented mappings in Table 9, enable consistent benchmarking of decoding robustness. We applied the best-performing model (T5 Model 3) under these conditions and conducted cross-domain tests, where training was performed on D1 and evaluation on D2, then reversing the setup with a random subset of D1 reserved for testing (Table 10). This evaluation intentionally excludes *emg2qwerty*, which was designed primarily to validate hardware-level interaction and thus contains mostly short (four-word) sequences with limited syntactic structure, which is appropriate for simple statistical baselines (e.g., *n*-grams). In contrast, D1 and D2 comprise longer, grammatically coherent sentences, providing a more challenging and representative testbed for cross-domain decoding. Across these conditions, the sentence decoder maintains low CER (< 2%) despite linguistic variability, indicating that the T5-based decoder is robust and well-suited for deployment beyond controlled lab settings.

Table 10. **Cross-Dataset Generalization.**

Train	Test	CER (%)
D1 (741)	D2 (584)	1.7
D2 (584)	D1 (300)	0.9

### Key Takeaway from RQ2

The MyoText framework generalizes effectively beyond the *emg2qwerty* dataset. It reconstructs longer, naturalistic sentences with high fidelity, remains robust under typing variability introduced by non-canonical finger-to-key mappings, and sustains performance when tested on unseen open-domain datasets. These results highlight the sentence decoder’s resilience to input noise and domain shift, underscoring its potential for deployment in diverse real-world scenarios.

### 5.3 RQ3: Analyzing *emg2qwerty* Dataset

We conduct an in-depth analysis to validate the quality and relevance of the *emg2qwerty* dataset used in our evaluation. It is a recently released large-scale dataset that has not yet been extensively studied. The dataset contains sEMG recordings collected with a wrist-mounted array while participants typed on a QWERTY keyboard. The corpus comprises sEMG and corresponding keystroke data from 108 participants, with prompts drawn from dictionaries and Wikipedia to ensure lexical and syntactic coverage. To assess suitability for our study, we analyze signal consistency and finger-specific patterns among users with high-quality tags from the dataset.

**Signal quality and finger-level consistency.** To verify signal stability, we computed RMS amplitude distributions for each finger over a 2 s window centered on each keystroke (1 s before and 1 s after). This window captures both pre-activation and relaxation phases, which lowers the median amplitude relative to peak contraction values. As shown in Fig. 9, median RMS amplitudes range from 10.6-11.0  $\mu\text{V}$  with standard deviations of 4.6-5.1  $\mu\text{V}$ . Interquartile ranges remain tight (approximately 5-15  $\mu\text{V}$ ), while higher-magnitude points (extending to 50–60  $\mu\text{V}$ ) correspond to key presses rather than statistical outliers. The coefficient of variation ( $\text{CV} = \sigma_{\text{RMS}}/\mu_{\text{RMS}}$ ) ranges from 42-47%, suggesting consistent scaling across fingers and systematic, not random, variability.

To quantify signal consistency, we calculated the signal-to-noise ratio (SNR) for each finger, defined as the inverse of the coefficient of variation ( $\text{SNR} = \mu_{\text{RMS}}/\sigma_{\text{RMS}}$ ). As shown in Fig. 10, all fingers exhibit consistent and repeatable signals, with SNR values between 2.12 and 2.37 (mean=2.3). Finger 3 has the highest SNR (2.37), indicating highly repeatable muscle activations, likely due to its independent motor control [38]. Finger 9 has the lowest SNR (2.12), which may result from its complex anatomy and great overlap with neighboring muscles [55].

These consistent amplitude distributions and SNR values confirm that the dataset captures stable, physiologically plausible muscle activation patterns with sufficient signal quality for reliable keystroke-level decoding

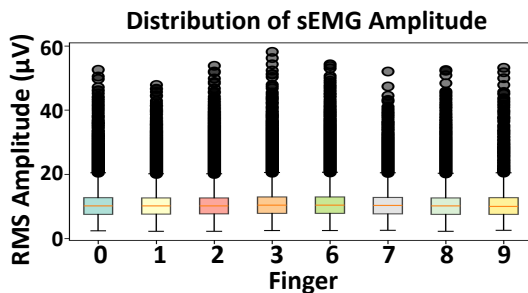


Fig. 9. **sEMG amplitudes by finger class.** Computed from 2 s windows centered on each keypress. Points above 40–50  $\mu\text{V}$  correspond to key presses rather than outliers.

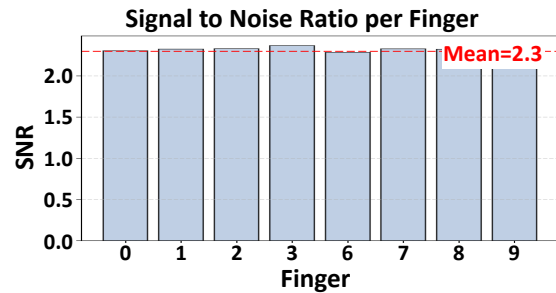


Fig. 10. **Within-class RMS stability ( $\mu/\sigma$ ).** Mean-to-std ratio per finger over 2 s windows; values cluster near 2.3, indicating consistent signal quality.

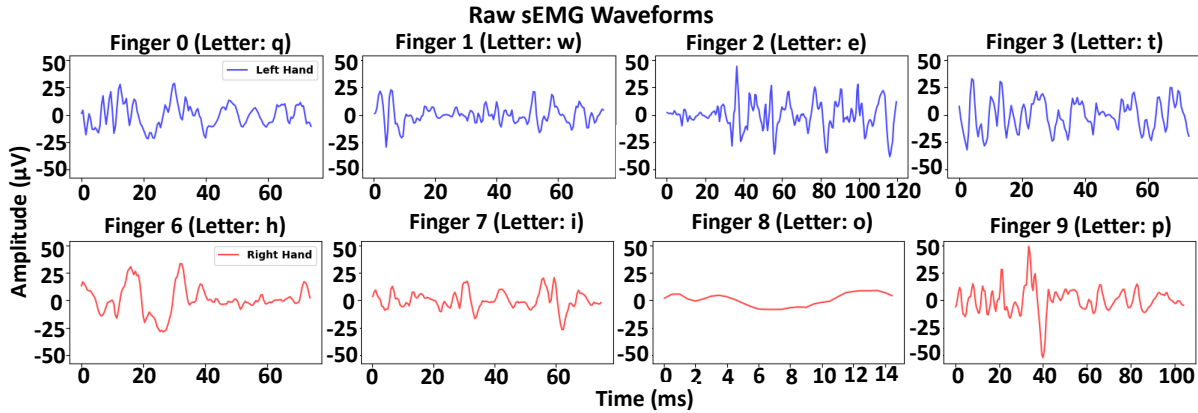


Fig. 11. **Finger-specific sEMG waveforms.** Averaged single-press waveforms show distinct temporal morphologies across fingers, supporting temporally-aware decoding.

**Finger-specific waveform morphology.** Beyond aggregate amplitude metrics, we examine whether individual fingers produce distinguishable temporal patterns. Fig. 11 shows raw sEMG for single keypresses across fingers 0-9. Waveforms exhibit apparent finger-specific differences in duration (15-110 ms), peak amplitude ( $\pm 20$ - $50 \mu V$ ), and frequency content. Finger 8 ('o') shows brief, smooth activation ( $\sim 15$  ms,  $\pm 20 \mu V$ ), while Finger 2 ('e') displays sustained high-frequency activity ( $\sim 110$  ms). Finger 9 ('p') reaches the highest amplitude ( $\pm 50 \mu V$ ), and Finger 6 ('h') shows dense transients. These distinct temporal signatures demonstrate finger-level discriminability and motivate temporal modeling approaches that capture waveform morphology rather than amplitude alone. These distinct temporal signatures qualitatively illustrate finger-level discriminability and motivate temporal modeling approaches that capture waveform morphology rather than amplitude alone.

#### Key takeaway for RQ3

The *emg2qwerty* dataset exhibits consistent signal quality and distinct finger-specific patterns in both amplitude and temporal domains. This stability and discriminability across users make it suitable for evaluating supervised keystroke decoding approaches.

#### 5.4 RQ4: Positioning MyoText within sEMG-to-Text Systems and Real-World Deployment

To evaluate the practical utility of MyoText, we situate it within prior sEMG-to-text literature and examine how its modular design supports deployment on contemporary wearable platforms.

**Existing Approaches of sEMG-to-text Systems.** Table 11 summarizes representative sEMG-to-text systems reported in the literature. While these studies differ in terms of datasets, vocabulary size, and task formulation, they collectively illustrate advancements in EMG-based text systems, ranging from gesture-driven interfaces to sentence-level decoding on compact wearable devices. Within this evolving landscape, MyoText contributes an expanded evaluation scale, with both MyoText and the *emg2qwerty* baseline tested on  $\geq 30$  participants. This broader cohort supports stronger insights into generalizability and user adaptation compared to the smaller-scale evaluations common in earlier work. On the *emg2qwerty* dataset—using a wrist-worn sEMG device and the same 30-user configuration—MyoText achieves a 5.4% character error rate (CER), whereas the method in [92] yields 64% CER (i.e., 36% per-character accuracy, since  $CER = 1 - \text{accuracy}$ ) under identical conditions (Table 11). This

Table 11. **sEMG-to-Text Landscape.** Representative systems reported in the literature. Metrics are shown as reported: Accuracy (Acc) indicates the fraction of correctly predicted characters, while Character Error Rate (CER) represents the fraction of incorrectly predicted characters ( $CER = 1 - Acc$ ).

System	Users	Channels	Device	Task	Metric
Sharma et al. [90]	10	2	BIOPAC	7 keys	92.7% Acc
Fu et al. [37]	–	8	Myo band	T9 gestures (9 keys)	85.9% Acc
Crouch et al. [20] <sup>‡</sup>	148k keys <sup>‡</sup>	32	Dual sleeves	Podcast transcription (full vocab)	91% Acc
Wang et al. [112]	–	32	16×16 band	30 symbols (26 letters + space/backspace/enter/period)	3.8% CER
Sivakumar et al. [92] <sup>†</sup>	108	32	Wrist band	Full sentences (26 keys, ~4 words per sentence)	52% CER
Sivakumar et al. [92] <sup>†</sup>	30*	32	Wrist Band	Full-sentence decoding (26 keys, ~4 words/sentence)	64% CER (36% Acc)
<b>MyoText (ours)<sup>†</sup></b>	<b>30</b>	<b>32</b>	<b>Wrist band</b>	<b>Full sentences (26 keys, ~4 words per sentence)</b>	<b>5.4% CER (94.6% Acc)</b>

Note: User cohorts are shown as reported (– = not specified). <sup>†</sup> denotes evaluation on the same dataset and hardware (*emg2qwerty*, 32-channel wrist band). \* indicates reimplement and re-evaluation on the 30-user subset used for MyoText. <sup>‡</sup> indicates keystrokes reported instead of participant count.

accuracy level aligns with our findings in RQ1 (§5.1), where letter classification achieved a similar accuracy range. Reported results in the broader literature span a range of system designs and evaluation setups. For example, Wang et al. [112] report a 3.8% CER on a 30-symbol set, and Crouch et al. [20] achieve 91% accuracy using dual-forearm sleeves for podcast transcription. Together, these works delineate the current performance envelope of sEMG-based decoding systems under diverse vocabulary sizes, datasets, and device configurations. The reduction in CER observed for MyoText reflects the efficacy of its modular framework, which integrates a physiological finger-motion classifier with a transformer-based sentence decoder. By decoupling physiological decoding from linguistic reasoning, the approach generalizes across users.

**Deployment Feasibility.** Beyond accuracy, the practical viability of sEMG-to-text systems depends on computational efficiency and real-time operation within the strict power and memory constraints of wearable devices. A monolithic end-to-end model that jointly decodes finger movements and generates text would exceed the compute and power budgets typical of wearables. Conversely, a cloud-only approach introduces privacy risks, network dependence, and latency [35, 51]. To address these challenges, MyoText adopts a split-execution design where the finger classifier can operate locally on the wearable device, while the transformer-based sentence decoder can run on a paired phone or edge processor. Profiling the two main components of MyoText shows that Step 2 (finger classifier) executes in ~60ms per sample, requiring only  $\approx 12$ MOPs and < 12MB of memory, which is well within interactive thresholds for contemporary wearables [63, 85, 112]. Modern edge NPUs deliver 38–80TOPS (Apple M4, Snapdragon X2 Elite) [4, 44, 65, 74], readily supporting this module on-device. Step 4 (transformer decoder) is computationally more intensive but is efficiently handled by mobile-class hardware. On an NVIDIA L4 GPU, inference runs at 18.851ms/token. Advances in quantization, kernel fusion, and attention caching now enable billion-parameter transformers to operate on mobile NPUs [12, 41, 66]. Commercial deployments (e.g., Apple ANE, Google on-device LLMs) already demonstrate low-latency text generation without that in cloud-independent.

Together, these results indicate that MyoText is deployable on current hardware: the finger classifier runs locally on the resource-constrained wearable, while the language model executes on a paired, resource-rich device such as a smartphone or edge processor.

#### Key Takeaway from RQ4

MyoText achieves an accuracy (5.4% CER) while offering key advantages, such as cross-user generalization and a physiologically grounded architecture. The finger classifier fits within on-wrist compute budgets, and the transformer decoder runs efficiently on paired smartphones, enabling practical, privacy-preserving sEMG text entry on current hardware.

## 6 Discussion and Future Work

MyoText introduces the first physiologically grounded approach to sEMG-based text decoding by explicitly modeling the relationship between muscular activation and typing behavior. Unlike prior end-to-end systems that directly map sEMG signals to letters, MyoText first predicts the active finger, which is a feature directly linked to EMG activity, before invoking a transformer-based language model for sentence decoding. This hierarchical design substantially reduces the effective search space of possible letters enabling the language model to operate within well-defined, context-aware constraints. The result is a decoding framework that couples physiological interpretability with linguistic fluency, achieving low character error rates while preserving computational efficiency suitable for wearable deployment.

However, several opportunities exist to strengthen our findings. First, while our evaluation uses a single dataset, it represents the most extensive available sEMG typing resource with 108 participants. Due to computational constraints, we evaluated our model on 30 users, which is a robust sample size that is larger than those used in many previous EMG typing studies. This sample size is justified by our modular framework, and the LOUO validation confirms consistent cross-user generalization. Our 30-user cohort with explicit LOUO evaluation matches or surpasses prior sEMG-to-text work (see Table 11). In future work, we will evaluate the full participant pool to validate generalizability further. Second, this work focuses on validating the core innovation of the MyoText framework rather than its end-to-end deployment. Future implementations incorporating real-time sEMG acquisition and on-device processing will provide crucial insights into system latency and power consumption for practical wearable deployment. Third, while we employ standardized QWERTY finger-key mappings, individual typing strategies vary considerably. Our experiments incorporate noise models to simulate these deviations, and the *emg2qwerty* dataset’s trained typists exhibit more consistent patterns than general users. A comprehensive survey of population-level finger-key preferences would enable more personalized decoding strategies. MyoText establishes a viable foundation for hands-free text input; the challenge ahead is scaling the data, refining the models, and validating the system outside controlled settings. MyoText’s flexibility suggests broad applications, including gesture interfaces, assistive technologies for motor impairments, and silent communication in noise-sensitive environments, providing a blueprint for next-generation biosignal-based human-computer interaction.

## 7 Conclusion

We presented MyoText, a physiologically grounded and modular sEMG-to-text decoding framework that integrates finger-level classification, ergonomically constrained letter mapping, and a transformer-based sentence generation model. Unlike prior monolithic or gesture-based systems, MyoText establishes a structured motor–linguistic hierarchy that mirrors the neuromuscular process of typing. Leveraging the *emg2qwerty* dataset, MyoText achieves 85.4% finger-classification accuracy and 5.4% character error rate (CER), demonstrating reliable decoding performance across users. This work represents a step toward scalable, keyboard-free communication interfaces,

advancing the practical realization of neural input for AR/VR environments, assistive technologies, and ubiquitous computing platforms.

## References

- [1] Bashaer A Al Abdullah, Ghada A Amoudi, and Hanan S Alghamdi. 2024. Advancements in sign language recognition: A comprehensive review and future prospects. *IEEE Access* 12 (2024), 128871–128895.
- [2] Muhammad Al-Ayyad, Hamza Abu Owida, Roberto De Fazio, Bassam Al-Naami, and Paolo Visconti. 2023. Electromyography monitoring systems in rehabilitation: A review of clinical applications, wearable devices and signal acquisition methodologies. *Electronics* 12, 7 (2023), 1520.
- [3] Christoph Amma, Thomas Krings, Jonas Böer, and Tanja Schultz. 2015. Advancing muscle-computer interfaces with high-density electromyography. In *Proceedings of the 33rd annual ACM conference on human factors in computing systems*. 929–938.
- [4] Apple Inc. 2024. Apple introduces M4 chip. Apple Newsroom. <https://www.apple.com/newsroom/2024/05/apple-introduces-m4-chip/>
- [5] P Artemiadis. 2012. EMG-based robot control interfaces: past, present and future. *Advances in Robotics & Automation* 1, 2 (2012), 1–3.
- [6] Stefan Costin Atitienei and Anca Marginean. 2024. Exploring the Limits of T5: Multitask Fine-Tuning for Reasoning, Summarization, Sentiment Analysis and Figurative Language Understanding. In *2024 IEEE 20th International Conference on Intelligent Computer Communication and Processing (ICCP)*. IEEE, 01–08.
- [7] Halim Wildan Awalurahman and Indra Budi. 2024. Automatic distractor generation in multiple-choice questions: A systematic literature review. *PeerJ Computer Science* 10 (2024), e2441.
- [8] Cord Bolte. 2025. Typing with 10 fingers quickly explained - TypingAcademy. <https://www.typing.academy/10-finger-typing> [Online; accessed 2025-04-14].
- [9] Dextina Alana Booker. 2020. *The future of fashion & human gesture control: exploration of a wearable communication device for sign language speakers*. Ph. D. Dissertation. Massachusetts Institute of Technology.
- [10] ChatSent12:online 2025. Chat Sentiment Dataset. <https://www.kaggle.com/datasets/nursyahrina/chat-sentiment-dataset> [Online; accessed 2025-09-26].
- [11] Baibhab Chatterjee, Pedram Mohseni, and Shreyas Sen. 2023. Bioelectronic sensor nodes for the internet of bodies. *Annual Review of Biomedical Engineering* 25, 1 (2023), 101–129.
- [12] Kevin Chen. 2025. Running a 7B Transformer on Your Phone: How Quantization is Pushing the Limits. AI in Plain English. <https://ai.plainenglish.io/running-a-7b-transformer-on-your-phone-how-quantization-is-pushing-the-limits-e70b3307595d>
- [13] Karen B. Chen, Kevin Ponto, Ross D. Tredinnick, and Robert G. Radwin. 2015. Virtual Exertions: Evoking the Sense of Exerting Forces in Virtual Reality Using Gestures and Muscle Activity. *Human Factors* 57, 4 (2015), 658–673. doi:10.1177/0018720814562231 arXiv:<https://doi.org/10.1177/0018720814562231> PMID: 25977324.
- [14] Yongming Chen, Haihong Zhang, Chuanchu Wang, Kai Keng Ang, Soon Huat Ng, Huiwen Jin, and Zhiping Lin. 2023. A hierarchical dynamic Bayesian learning network for EMG-based early prediction of voluntary movement intention. *Scientific Reports* 13, 1 (2023), 4730.
- [15] Manisha Choudhary, Monika Lokhande, Rushikesh Borse, and Avinash Bhute. 2022. A machine learning approach to aid paralysis patients using EMG signals. In *Advanced Data Mining Tools and Methods for Social Computing*. Elsevier, 107–125.
- [16] Meghna Roy Chowdhury, Archisman Ghosh, Md Faizul Bari, and Shreyas Sen. 2024. Leveraging Ultra-Low-Power Wearables Using Distributed Neural Networks. In *2024 IEEE 20th International Conference on Body Sensor Networks (BSN)*. IEEE, 1–4.
- [17] Rubana H Chowdhury, Mamun BI Reaz, Mohd Alauddin Bin Mohd Ali, Ashrif AA Bakar, Kalaivani Chellappan, and Tae G Chang. 2013. Surface electromyography signal processing and classification techniques. *Sensors* 13, 9 (2013), 12431–12466.
- [18] Andrea Cimolati, Josephus JM Driessen, Leonardo S Mattos, Elena De Momi, Matteo Laffranchi, and Lorenzo De Michieli. 2022. EMG-driven control in lower limb prostheses: A topic-based systematic review. *Journal of NeuroEngineering and Rehabilitation* 19, 1 (2022), 43.
- [19] Jan Pieter Clarys and Jan Cabri. 1993. Electromyography and the study of sports movements: a review. *Journal of sports sciences* 11, 5 (1993), 379–448.
- [20] Michael S Crouch, Mingde Zheng, and Michael S Eggleston. 2021. Natural typing recognition via surface electromyography. *arXiv preprint arXiv:2109.10743* (2021).
- [21] Carlo J De Luca. 2002. Surface electromyography: Detection and recording. *DelSys Incorporated* 10, 2 (2002), 1–10.
- [22] Riccardo Di Giminiani, Marco Cardinale, Marco Ferrari, and Valentina Quaresima. 2020. Validation of fabric-based thigh-wearable EMG sensors and oximetry for monitoring quadriceps activity during strength and endurance exercises. *Sensors* 20, 17 (2020), 4664.
- [23] Denise K Donica, Peter Giroux, and Amber Faust. 2018. Keyboarding instruction: Comparison of techniques for improved keyboarding skills in elementary students. *Journal of Occupational Therapy, Schools, & Early Intervention* 11, 4 (2018), 396–410.
- [24] Yu Du, Wenguang Jin, Wentao Wei, Yu Hu, and Weidong Geng. 2017. Surface EMG-based inter-session gesture recognition enhanced by deep domain adaptation. *Sensors* 17, 3 (2017), 458.

- [25] Anany Dwivedi, Yongje Kwon, and Minas Liarokapis. 2020. Emg-based decoding of manipulation motions in virtual reality: Towards immersive interfaces. In *2020 IEEE International Conference on Systems, Man, and Cybernetics (SMC)*. IEEE, 3296–3303.
- [26] dwyl. 2025. english-words/words\_alpha.txt at master · dwyl/english-words · GitHub. [https://github.com/dwyl/english-words/blob/master/words\\_alpha.txt](https://github.com/dwyl/english-words/blob/master/words_alpha.txt) [Online; accessed 2025-04-28].
- [27] Jonathan Eby, Moshe Beutel, David Koivisto, Idan Achituve, Ethan Fetaya, and José Zariffa. 2025. Electromyographic typing gesture classification dataset for neurotechnological human-machine interfaces. *Scientific Data* 12, 1 (2025), 440.
- [28] Oussama EL GHOUL, Mohamed JEMNI, et al. 2024. Design and Implementation of an EMG-Based Communication Interface for Enhancing Interaction with Deaf Individuals. *Journal of Information Sciences* 23, 2 (2024), 1–20.
- [29] Electrom90:online. 2023. Electromyography (EMG) | Johns Hopkins Medicine. <https://www.hopkinsmedicine.org/health/treatment-tests-and-therapies/electromyography-emg> [Online; accessed 2025-04-10].
- [30] facebookresearch. 2025. GitHub - facebookresearch/emg2qwerty: A surface electromyographic (sEMG) touch typing dataset with baselines. <https://arxiv.org/abs/2410.20081>. <https://github.com/facebookresearch/emg2qwerty> [Online; accessed 2025-04-29].
- [31] Yongxin Fan, Qian Tang, Yangming Guo, and Yifei Wei. 2024. BiLSTM-MLAM: a multi-scale time series prediction model for sensor data based on Bi-LSTM and local attention mechanisms. *Sensors* 24, 12 (2024), 3962.
- [32] Yongfei Feng, Mingwei Zhong, Xusheng Wang, Hao Lu, Hongbo Wang, Pengcheng Liu, and Luige Vladareanu. 2021. Active triggering control of pneumatic rehabilitation gloves based on surface electromyography sensors. *PeerJ Computer Science* 7 (2021), e448.
- [33] ELISABETH FERNSTRÖM, Mats O Ericson, and HANS MALKER. 1994. Electromyographic activity during typewriter and keyboard use. *Ergonomics* 37, 3 (1994), 477–484.
- [34] T Finni, Min Hu, P Kettunen, T Vilavuo, and S Cheng. 2007. Measurement of EMG activity with textile electrodes embedded into clothing. *Physiological measurement* 28, 11 (2007), 1405.
- [35] Fiveable. 2024. Power Consumption Challenges in Edge Devices. Fiveable Study Guide. <https://fiveable.me/edge-ai-and-computing/unit-8/power-consumption-challenges-edge-devices/study-guide/kU7ZtkGCmjmI4oOW>
- [36] Adam Freed, Adrian DC Chan, Edward D Lemaire, and Avi Parush. 2011. Wearable EMG analysis for rehabilitation (WEAR)-surface electromyography in clinical gait analysis. In *2011 IEEE International Symposium on Medical Measurements and Applications*. IEEE, 601–604.
- [37] Zongkai Fu, Huiyong Li, Zhenchao Ouyang, Xuefeng Liu, and Jianwei Niu. 2020. Typing everywhere with an EMG keyboard: A novel MYO armband-based HCI tool. In *International Conference on Algorithms and Architectures for Parallel Processing*. Springer, 247–261.
- [38] Andrew J Fuglevand, Vaughan G Macefield, and Brenda Bigland-Ritchie. 1999. Force-frequency and fatigue properties of motor units in muscles that control digits of the human hand. *Journal of neurophysiology* 81, 4 (1999), 1718–1729.
- [39] Donald R Gentner. 1983. Keystroke timing in transcription typing. In *Cognitive aspects of skilled typewriting*. Springer, 95–120.
- [40] Vidhi Gohel and Ninad Mehendale. 2020. Review on electromyography signal acquisition and processing. *Biophysical reviews* 12, 6 (2020), 1361–1367.
- [41] Dibakar Gope, David Mansell, et al. 2025. Highly Optimized Kernels and Fine-Grained Codebooks for LLM Inference on Arm CPUs. *arXiv preprint arXiv:2501.00032* (2025).
- [42] Reed D Gurchiek, Nicole Donahue, Niccolo M Fiorentino, and Ryan S McGinnis. 2021. Wearables-only analysis of muscle and joint mechanics: an EMG-driven approach. *IEEE Transactions on Biomedical Engineering* 69, 2 (2021), 580–589.
- [43] Awni Hannun, Ann Lee, Qiantong Xu, and Ronan Collobert. 2019. Sequence-to-sequence speech recognition with time-depth separable convolutions. *arXiv preprint arXiv:1904.02619* (2019).
- [44] Adam Hartley. 2024. TOPS explained – exactly how powerful is Apple’s new M4 iPad chip? TechRadar. <https://www.techradar.com/computing/artificial-intelligence/tops-explained-exactly-how-powerful-is-apples-new-m4-ipad-chip>
- [45] heathera. 2025. Meta Ray-Ban Display: AI Glasses With an EMG Wristband. <https://about.fb.com/news/2025/09/meta-ray-ban-display-ai-glasses-emg-wristband/> [Online; accessed 2025-09-29].
- [46] Matthias Janke and Lorenz Diener. 2017. EMG-to-speech: Direct generation of speech from facial electromyographic signals. *IEEE/ACM Transactions on Audio, Speech, and Language Processing* 25, 12 (2017), 2375–2385.
- [47] Szu-Chen Stan Jou, Tanja Schultz, Matthias Walliczek, Florian Kraft, and Alex Waibel. 2006. Towards continuous speech recognition using surface electromyography. In *Interspeech*. 573–576.
- [48] P Kaifosh and T Reardon. 2024. A generic noninvasive neuromotor interface for human-computer interaction. *bioRxiv* (2024).
- [49] Victor Kartsch, Simone Benatti, Mattia Mancini, Michele Magno, and Luca Benini. 2018. Smart wearable wristband for EMG based gesture recognition powered by solar energy harvester. In *2018 IEEE International Symposium on Circuits and Systems (ISCAS)*. IEEE, 1–5.
- [50] Diederik P Kingma and Jimmy Ba. 2014. Adam: A method for stochastic optimization. *arXiv preprint arXiv:1412.6980* (2014).
- [51] Kisaco Research. 2024. A Practical Guide to Edge AI Power Efficiency. Kisaco Research. [https://www.kisacoresearch.com/sites/default/files/documents/halio\\_whitepaper\\_edge\\_ai\\_power\\_efficiency.pdf](https://www.kisacoresearch.com/sites/default/files/documents/halio_whitepaper_edge_ai_power_efficiency.pdf)
- [52] Heli Koskimäki, Pekka Siirtola, and Juha Rönning. 2017. Myogym: introducing an open gym data set for activity recognition collected using myo armband. In *Proceedings of the 2017 ACM international joint conference on pervasive and ubiquitous computing and proceedings*

- of the 2017 ACM international symposium on wearable computers. 537–546.
- [53] Yi-Liang Kuo, Pei-San Wang, Po-Yen Ko, Kuo-Yuan Huang, and Yi-Ju Tsai. 2019. Immediate effects of real-time postural biofeedback on spinal posture, muscle activity, and perceived pain severity in adults with neck pain. *Gait & posture* 67 (2019), 187–193.
- [54] Meta Reality Labs. 2021. Introducing a wrist-based wearable for neural input. <https://tech.fb.com/inside-facebook-reality-labs-wrist-based-interaction>. Accessed April 2025.
- [55] JNAL Leijnse, PM Quesada, and CW Spoor. 2010. Kinematic evaluation of the finger’s interphalangeal joints coupling mechanism—variability, flexion–extension differences, triggers, locking swanneck deformities, anthropometric correlations. *Journal of biomechanics* 43, 12 (2010), 2381–2393.
- [56] Alessandro Leone, Gabriele Rescio, Lucia Giampetruzzi, and Pietro Siciliano. 2019. Smart EMG-based socks for leg muscles contraction assessment. In *2019 IEEE International Symposium on Measurements & Networking (M&N)*. IEEE, 1–6.
- [57] Alessandro Leone, Gabriele Rescio, and Pietro Siciliano. 2017. Fall risk evaluation by surface electromyography technology. In *2017 International Conference on Engineering, Technology and Innovation (ICE/ITMC)*. IEEE, 1092–1095.
- [58] Dongming Li, Linnan Huang, Yangrong Wen, Yueming Gao, Željka Lučev Vasić, Mario Cifrek, and Min Du. 2020. Analysis of electrical impedance myography electrodes configuration for local muscle fatigue evaluation based on finite element method. *IEEE access* 8 (2020), 172233–172243.
- [59] Mengfang Li, Yuanyuan Jiang, Yanzhou Zhang, and Haisheng Zhu. 2023. Medical image analysis using deep learning algorithms. *Frontiers in public health* 11 (2023), 1273253.
- [60] Na Li, Rui Zhou, Bharath Krishna, Ashirbad Pradhan, Hyowon Lee, Jiayuan He, and Ning Jiang. 2024. Non-invasive techniques for muscle fatigue monitoring: a comprehensive survey. *Comput. Surveys* 56, 9 (2024), 1–40.
- [61] Jintao Ling and Muhammad Afzaal. 2024. Automatic question-answer pairs generation using pre-trained large language models in higher education. *Computers and Education: Artificial Intelligence* 6 (2024), 100252.
- [62] Simone Maragliulo, Pedro Filipe Alhais Lopes, Luis Bica Osório, Anibal T De Almeida, and Mahmoud Tavakoli. 2019. Foot gesture recognition through dual channel wearable EMG System. *IEEE Sensors Journal* 19, 22 (2019), 10187–10197.
- [63] Jean-Mathieu Maro et al. 2024. Helios: An extremely low power event-based gesture recognition for always-on smart eyewear. *arXiv preprint arXiv:2407.05206* (2024).
- [64] Alaa Marshan, Anwar Nais Almutairi, Athina Ioannou, David Bell, Asmat Monaghan, and Mahir Arzoky. 2024. MedT5SQL: a transformers-based large language model for text-to-SQL conversion in the healthcare domain. *Frontiers in Big Data* 7 (2024), 1371680.
- [65] Jon Martindale. 2025. Snapdragon X2 Elite vs Snapdragon X Elite: Here’s what’s new. Tom’s Guide. <https://www.tomsguide.com/computing/cpus/snapdragon-x2-elite-vs-snapdragon-x-elite-heres-whats-new>
- [66] Meta AI. 2024. Introducing quantized Llama models with increased speed and a reduced memory footprint. Meta AI Blog. <https://ai.meta.com/blog/meta-llama-quantized-lightweight-models/>
- [67] Kerry R Mills. 2005. The basics of electromyography. *Journal of Neurology, Neurosurgery & Psychiatry* 76, suppl 2 (2005), ii32–ii35.
- [68] Ninapro25:online 2025. Ninapro. <https://ninapro.hevs.ch/> [Online; accessed 2025-04-14].
- [69] NLTKSamp10:online 2025. NLTK :: Sample usage for corpus. <https://www.nltk.org/howto/corpus.html> [Online; accessed 2025-04-28].
- [70] Mina Nouredanesh, Sunil L Kukreja, and James Tung. 2016. Detection of compensatory balance responses using wearable electromyography sensors for fall-risk assessment. In *2016 38th Annual International Conference of the IEEE Engineering in Medicine and Biology Society (EMBC)*. IEEE, 1680–1683.
- [71] Jan Noyes. 1983. The QWERTY keyboard: A review. *International Journal of Man-Machine Studies* 18, 3 (1983), 265–281.
- [72] OrionAIG74:online 2025. Orion AI Glasses: The Future of AR Glasses Technology | Meta. <https://about.meta.com/realitylabs/orion/> [Online; accessed 2025-04-08].
- [73] Ted Pedersen, Siddharth Patwardhan, Jason Michelizzi, et al. 2004. WordNet:: Similarity-Measuring the Relatedness of Concepts.. In *AAAI*, Vol. 4. 25–29.
- [74] Tom Petri. 2025. Snapdragon X2 Elite Extreme crushes Apple M4, Intel, and AMD in new benchmarks. Windows Central. <https://www.windowscentral.com/hardware/qualcomm/snapdragon-x2-elite-extreme-crushes-apple-m4-intel-and-amd-in-new-benchmarks>
- [75] Carlos G Pinheiro Jr, Eduardo LM Naves, Pierre Pino, Etienne Losson, Adriano O Andrade, and Guy Bourhis. 2011. Alternative communication systems for people with severe motor disabilities: a survey. *Biomedical engineering online* 10, 1 (2011), 31.
- [76] M Raez, M Hussain, and F Mohd-Yasin. 2006. Techniques of EMG signal analysis: Detection, processing, classification and applications. Retrieved October 16, 2018.
- [77] Colin Raffel, Noam Shazeer, Adam Roberts, Katherine Lee, Sharan Narang, Michael Matena, Yanqi Zhou, Wei Li, and Peter J Liu. 2020. Exploring the limits of transfer learning with a unified text-to-text transformer. *Journal of Machine Learning Research* 21, 140 (2020), 1–67.
- [78] Ismo Rakkolainen, Ahmed Farooq, Jari Kangas, Jaakko Hakulinen, Jussi Rantala, Markku Turunen, and Roope Raisamo. 2021. Technologies for multimodal interaction in extended reality—a scoping review. *Multimodal Technologies and Interaction* 5, 12 (2021), 81.

- [79] Randomen9:online 2025. Random english sentences. <https://www.kaggle.com/datasets/nikitricky/random-english-sentences> [Online; accessed 2025-09-26].
- [80] Gundala Jhansi Rani, Mohammad Farukh Hashmi, and Aditya Gupta. 2023. Surface electromyography and artificial intelligence for human activity recognition—a systematic review on methods, emerging trends applications, challenges, and future implementation. *IEEE access* 11 (2023), 105140–105169.
- [81] Seema Rawat, Somya Vats, and Praveen Kumar. 2016. Evaluating and exploring the MYO ARMBAND. In *2016 International Conference System Modeling & Advancement in Research Trends (SMART)*. IEEE, 115–120.
- [82] Devon I Rubin. 2019. Needle electromyography: Basic concepts. *Handbook of clinical neurology* 160 (2019), 243–256.
- [83] Tara N Sainath, Oriol Vinyals, Andrew Senior, and Haşim Sak. 2015. Convolutional, long short-term memory, fully connected deep neural networks. In *2015 IEEE international conference on acoustics, speech and signal processing (ICASSP)*. Ieee, 4580–4584.
- [84] Christian Sax, Hannes Lau, and Elaine Lawrence. 2011. Liquid Keyboard: An ergonomic, adaptive QWERTY keyboard for touchscreens and surfaces. *feedback* 64 (2011), 19.
- [85] Md Abu Sayeed and Fatahia Nasrin. 2023. An edge-computing platform for low-latency and low-power wearable medical devices for epilepsy. In *2023 IEEE Texas Symposium on Wireless and Microwave Circuits and Systems (WMCS)*. IEEE, 1–4.
- [86] Ovishake Sen, Anna M Sheehan, Pranay R Raman, Kabir S Khara, Adam Khalifa, and Baibhab Chatterjee. 2023. Machine-learning methods for speech and handwriting detection using neural signals: a review. *Sensors* 23, 12 (2023), 5575.
- [87] Shreyas Sen and Arunashish Datta. 2024. Human-Inspired Distributed Wearable AI. In *Proceedings of the 61st ACM/IEEE Design Automation Conference*. 1–4.
- [88] Shreyas Sen and Arunashish Datta. 2024. Invited: Human-Inspired Distributed Wearable AI. In *Proceedings of the 61st ACM/IEEE Design Automation Conference (San Francisco, CA, USA) (DAC '24)*. Association for Computing Machinery, New York, NY, USA, Article 364, 4 pages. doi:10.1145/3649329.3663513
- [89] Mehran Shabanpour, Kasra Rad, Sadaf Khademi, and Arash Mohammadi. 2025. MoEMba: A Mamba-based Mixture of Experts for High-Density EMG-based Hand Gesture Recognition. *arXiv preprint arXiv:2502.17457* (2025).
- [90] Rajneesh Sharma and Amit Kukker. 2017. Neural reinforcement learning based identifier for typing keys using forearm EMG signals. In *Proceedings of the 9th International Conference on Signal Processing Systems*. 225–229.
- [91] Guy G Simoneau, Richard W Marklin, and Joseph E Berman. 2003. Effect of computer keyboard slope on wrist position and forearm electromyography of typists without musculoskeletal disorders. *Physical Therapy* 83, 9 (2003), 816–830.
- [92] Viswanath Sivakumar, Jeffrey Seely, Alan Du, Sean Bittner, Adam Berenzweig, Anuoluwapo Bolarinwa, Alex Gramfort, and Michael Mandel. 2024. emg2qwerty: A large dataset with baselines for touch typing using surface electromyography. *Advances in Neural Information Processing Systems* 37 (2024), 91373–91389.
- [93] Andreia SP Sousa, Andreia Noites, Rui Vilarinho, and Rubim Santos. 2023. Long-term electrode–skin impedance variation for electromyographic measurements. *Sensors* 23, 20 (2023), 8582.
- [94] LV Srinivas, R Shiva Shankar, N Deshai, K Sravani, and V Maheswararao. 2024. Empowering Inclusive Communication: Advancements in Wearable Technology with GloSign—A Glove-Based Solution for Seamless Sign Language Interaction. In *Algorithms in Advanced Artificial Intelligence*. CRC Press, 492–501.
- [95] Erik Stålberg and Peter Dioszeghy. 1991. Scanning EMG in normal muscle and in neuromuscular disorders. *Electroencephalography and Clinical Neurophysiology/Evoked Potentials Section* 81, 6 (1991), 403–416.
- [96] Abdulhamit Subasi. 2013. Classification of EMG signals using PSO optimized SVM for diagnosis of neuromuscular disorders. *Computers in biology and medicine* 43, 5 (2013), 576–586.
- [97] S Sudarsan, IEEE Student Member, and E Chandra Sekaran. 2012. Design and development of EMG controlled prosthetics limb. *Procedia engineering* 38 (2012), 3547–3551.
- [98] Gabriel Synnaeve, Qiantong Xu, Jacob Kahn, Tatiana Likhomanenko, Edouard Grave, Vineel Pratap, Anuroop Sriram, Vitaliy Liptchinsky, and Ronan Collobert. 2019. End-to-end asr: from supervised to semi-supervised learning with modern architectures. *arXiv preprint arXiv:1911.08460* (2019).
- [99] T511:online 2025. T5. [https://huggingface.co/docs/transformers/en/model\\_doc/t5](https://huggingface.co/docs/transformers/en/model_doc/t5) [Online; accessed 2025-04-29].
- [100] Keras Team. 2025. ReduceLRonPlateau. [https://keras.io/api/callbacks/reduce\\_lr\\_on\\_plateau/](https://keras.io/api/callbacks/reduce_lr_on_plateau/) [Online; accessed 2025-04-29].
- [101] Shi-Liu Tian, Yu Liu, Li Li, Wei-Jie Fu, and Chien-Hua Peng. 2010. Mechanomyography is more sensitive than EMG in detecting age-related sarcopenia. *Journal of biomechanics* 43, 3 (2010), 551–556.
- [102] Dennis Tkach, He Huang, and Todd A Kuiken. 2010. Study of stability of time-domain features for electromyographic pattern recognition. *Journal of neuroengineering and rehabilitation* 7 (2010), 1–13.
- [103] Contributors to Wikimedia projects. 2004. Touch typing - Wikipedia. [https://en.wikipedia.org/wiki/Touch\\_typing?utm\\_source=chatgpt.com](https://en.wikipedia.org/wiki/Touch_typing?utm_source=chatgpt.com) [Online; accessed 2025-09-10].
- [104] Cinthya Lourdes Toledo-Peral, Gabriel Vega-Martinez, Jorge Airy Mercado-Gutiérrez, Gerardo Rodriguez-Reyes, Arturo Vera-Hernandez, Lorenzo Leija-Salas, and Josefina Gutierrez-Martinez. 2022. Virtual/augmented reality for rehabilitation applications using electromyography as control/biofeedback: systematic literature review. *Electronics* 11, 14 (2022), 2271.

- [105] TypingLe73:online 2025. Typing Lessons - Typing Basics Part 2 - finger assignment on keyboard. <https://www.learn2type.com/typingtest/lessons/typingkeyboards.cfm> [Online; accessed 2025-04-14].
- [106] Hisao Usui and Kanako Komiya. 2023. Translation from Historical to Contemporary Japanese Using Japanese T5. In *Proceedings of the Joint 3rd International Conference on Natural Language Processing for Digital Humanities and 8th International Workshop on Computational Linguistics for Uralic Languages*. 27–35.
- [107] A Prasad Vinod and Chai Yee Da. 2013. An integrated surface EMG data acquisition system for sports medicine applications. In *2013 7th International Symposium on Medical Information and Communication Technology (ISMICT)*. IEEE, 98–102.
- [108] Michael Wand and Tanja Schultz. 2011. Session-independent EMG-based Speech Recognition.. In *Biosignals*. 295–300.
- [109] Alex Wang, Yada Pruksachatkun, Nikita Nangia, Amanpreet Singh, Julian Michael, Felix Hill, Omer Levy, and Samuel Bowman. 2019. Superglue: A stickier benchmark for general-purpose language understanding systems. *Advances in neural information processing systems* 32 (2019).
- [110] Alex Wang, Amanpreet Singh, Julian Michael, Felix Hill, Omer Levy, and Samuel R Bowman. 2018. GLUE: A multi-task benchmark and analysis platform for natural language understanding. *arXiv preprint arXiv:1804.07461* (2018).
- [111] Jinqiang Wang, Dianguo Cao, Yang Li, Jiashuai Wang, and Yuqiang Wu. 2022. Multi-user motion recognition using sEMG via discriminative canonical correlation analysis and adaptive dimensionality reduction. *Frontiers in Neurobotics* 16 (2022), 997134.
- [112] Yi Wang, Youhao Wang, Ruilin Zhao, Yue Shi, and Yingnan Bian. 2024. Efficient Electromyography-Based Typing System: Towards a Novel Approach to HCI Text Input. In *2024 46th Annual International Conference of the IEEE Engineering in Medicine and Biology Society (EMBC)*. IEEE, 1–5.
- [113] Wearable26:online 2025. Wearable Technology | Myontec. <https://www.myontec.com/> [Online; accessed 2025-04-08].
- [114] WhereSho97:online 2025. Where Should Fingers Be Placed on the Keyboard? <https://www.computerhope.com/issues/ch001346.htm> [Online; accessed 2025-04-14].
- [115] Shumin Zhai and Per Ola Kristensson. 2012. The word-gesture keyboard: reimagining keyboard interaction. *Commun. ACM* 55, 9 (2012), 91–101.
- [116] Mingrui Ray Zhang, Shumin Zhai, and Jacob O Wobbrock. 2022. TypeAnywhere: A QWERTY-based text entry solution for ubiquitous computing. In *Proceedings of the 2022 CHI Conference on Human Factors in Computing Systems*. 1–16.
- [117] Qingqing Zhao, Yuhan Xia, Yunfei Long, Ge Xu, and Jia Wang. 2025. Leveraging sensory knowledge into Text-to-Text Transfer Transformer for enhanced emotion analysis. *Information Processing & Management* 62, 1 (2025), 103876.
- [118] Ping Zhou, Madeleine M Lowery, Kevin B Englehart, He Huang, Guanglin Li, Levi Hargrove, Julius PA Dewald, and Todd A Kuiken. 2007. Decoding a new neural-machine interface for control of artificial limbs. *Journal of neurophysiology* 98, 5 (2007), 2974–2982.